ENERGETIC AND ECONOMIC INVESTIGATION OF SOLAR ORGANIC RANKINE CYCLE İNTEGRATED WITH AN ABSORPTION REFRIGERATION SYSTEM FOR GENERATION POWER AND COOLING APPLICATIONS

2024
MASTER THESIS
MECHANICAL ENGINEERING

Muhamad REFAAI

Thesis Advisor
Assist. Prof. Dr. Abdulrazzak A. S. AKROOT

ENERGETIC AND ECONOMIC INVESTIGATION OF SOLAR ORGANIC RANKINE CYCLE İNTEGRATED WITH AN ABSORPTION REFRIGERATION SYSTEM FOR GENERATION POWER AND COOLING APPLICATIONS

Muhamad REFAAI

Thesis Advisor
Assist. Prof. Dr. Abdulrazzak A. S. AKROOT

T.C.
Karabuk University
Institute of Graduate Programs
Department of Mechanical Engineering
Prepared as
Master Thesis

KARABUK
April 2024

I certify that in my opinion the thesis submitted by Muhamad REFAAI titled "ENERGETIC AND ECONOMIC INVESTIGATION OF SOLAR ORGANIC RANKINE CYCLE İNTEGRATED WITH AN ABSORPTION REFRIGERATION SYSTEM FOR GENERATION POWER AND COOLING APPLICATIONS" is fully adequate in scope and in quality as a thesis for the degree of Master of Science.

Assist. Prof. Dr. Abdulrazzak Ahmed Saleh AKROOT ....

Thesis Advisor, Department of Mechanical Engineering

This thesis is accepted by the examining committee with a unanimous vote in the Department of Mechanical Engineering as a Master of Science thesis. April 16, 2024

Examining Committee Members (Institutions)   Signature

Chairman : Assist. Prof. Dr. Khaled M.N. CHAHROUR (KBU)   ....

Member   : Assoc. Prof. Dr. Hasanain Adnan Abdul WAHHAB (UOT).......................

Member   : Assist. Prof. Dr. Abdulrazzak AKROOT (KBU)   ....

The degree of Master of Science by the thesis submitted is approved by the Administrative Board of the Institute of Graduate Programs, Karabuk University.

Assoc. Prof. Dr. Zeynep ÖZCAN   ....

Director of the Institute of Graduate Programs

ii

ABSTRACT

M. Sc. Thesis

ENERGETIC AND ECONOMIC INVESTIGATION OF SOLAR ORGANIC RANKINE CYCLE İNTEGRATED WITH AN ABSORPTION REFRIGERATION SYSTEM FOR GENERATION POWER AND COOLING APPLICATIONS

Muhamad REFAAI

Karabük University
Institute of Graduate Programs
Department of Mechanical Engineering

Thesis Advisor:
Assist. Prof. Dr. Abdulrazzak Ahmed Saleh AKROOT
April 2024, 55 pages

The present study presents a simulation analysis that precisely investigates the thermodynamic and exergoeconomic elements of a solar-powered trigeneration system that generates electricity, heat, and cooling (CCHP) in Antalya, Turkey. The system utilizes parabolic trough collectors that use Therminol 66 to power an organic Rankine cycle and an absorption refrigeration system. The investigation was carried out under steady-state conditions, with a model constructed using Engineering Equation Solver (EES). Energy, exergy, and exergoeconomic assessments measure system performance, with R245fa and octane serving as working fluids in the organic Rankine cycle. A parametric analysis of the system is performed to evaluate how different parameters impact power generation, cooling, and heating output, the total cost rate, the system's thermal and exergy efficiency, and exergy destruction. The following

characteristics were assessed: the degree of superheating, the pressure at the turbine inlet, and the level of solar beam irradiation. The R245fa-based CCHP system generates 232.5 kW of electricity, 716.7 kW of cooling, 2225 kW of heating, 86.89% of thermal efficiency, 16.26% of exergy efficiency, and an overall cost rate of 66.12 $/h. Furthermore, the exergoeconomic factor is 72.12%, and the carbon footprint is 0.195 kg CO_2/kWh under ideal design conditions. The butane-powered CCHP system has an electrical output of 221.8 kW, a cooling production capacity of 745.4 kW, a heating production capacity of 2197 kW, a thermal efficiency of 86.44%, an exergy efficiency of 15.73%, a total cost rate of 63.06 $/h, an exergoeconomic factor of 70.86%, and the carbon footprint is 0.223 kg CO_2/kWh.

ÖZET

Yüksek Lisans Tezi

GÜNEŞ ENERJİSİ İLE ÇALIŞAN ORGANİK RANKİNE ÇEVRİMİNİN SOĞUTMA SİSTEMİ İLE ENTEGRASYONUNUN ENERJİ VE EKONOMİK ANALİZİ: GÜÇ ÜRETİMİ VE SOĞUTMA UYGULAMALARI

Muhamad REFAAI

Karabük Üniversitesi
Lisansüstü Eğitim Enstitüsü
Makine Mühendisliği Bölümü

Tez Danışmanı:
Dr. Öğr. Üyesi Abdulrazzak Ahmed Saleh AKROOT
Nisan 2024, 55 sayfa

Bu çalışma, Antalya, Türkiye'de elektrik, ısı ve soğutma (CCHP) üreten güneş enerjili bir trigenerasyon sisteminin termodinamik ve eksergoekonomik unsurlarını detaylı bir şekilde inceleyen bir simülasyon analizi sunmaktadır. Sistem, Therminol 66 kullanarak güneş enerjisi toplayan parabolik oluk kolektörlerini kullanarak organik Rankine çevrimi ve bir absorbsiyon soğutma sistemi ile çalışmaktadır. Araştırma, Engineering Equation Solver (EES) kullanılarak oluşturulan bir model ile durağan durum koşulları altında gerçekleştirilmiştir. Enerji, ekserji ve eksergoekonomik değerlendirmeler sistemin performansını ölçmekte olup, organik Rankine çevriminde çalışma sıvıları olarak R245fa ve oktan kullanılmıştır. Sistemin farklı parametrelerin güç üretimi, soğutma ve ısıtma çıktısı, toplam maliyet oranı, sistemin termal ve ekserji verimliliği ve ekserji yıkımı üzerindeki etkilerini değerlendirmek için bir parametrik analiz yapılmıştır. Değerlendirilen özellikler arasında türbin girişindeki basınç, süper ısıtma

derecesi ve güneş ışını şiddeti bulunmaktadır. R245fa tabanlı CCHP sistemi ideal tasarım koşulları altında 232.5 kW elektrik, 716.7 kW soğutma, 2225 kW ısıtma üretmekte, %86.89 termal verimlilik, %16.26 ekserji verimliliği ve saatte 66.12 $ toplam maliyet oranına sahiptir. Ayrıca, eksergoekonomik faktör %72.12 ve karbon ayak izi 0.195 kg CO_2/kWh'dır. Bütanla çalışan CCHP sistemi ise 221.8 kW elektrik, 745.4 kW soğutma kapasitesi, 2197 kW ısıtma kapasitesi, %86.44 termal verimlilik, %15.73 ekserji verimliliği, saatte 63.06 $ toplam maliyet oranına, %70.86 eksergoekonomik faktöre ve 0.223 kg CO_2/kWh karbon ayak izine sahiptir.

Anahtar Kelimeler : Trigenerasyon; Organik Rankine Çevrimi; Enerji ve Ekserji; Eksergoekonomik Analiz; Güneş Parabolik Oluk Güneş Kolektörleri.

Bilim Kodu : 91436

ACKNOWLEDGMENT

The completion of this thesis would not have been possible without the grace of the Almighty Allah, the Most Merciful and Beneficent, who showered me with His plentiful blessings.

I would like to take this opportunity to extend my deepest appreciation to my advisor, Assist. Prof. Dr. Abdulrazzak Ahmed Saleh AKROOT, for his immense support, motivation, and guidance in helping me finish this endeavor of mine. I would like to thank him also for helping me learn EES simulation tool.

The completion of this work would not have been possible without the love and support of my family and friends. The names are too numerous to mention but I will keep it short and simple. I would like to thank my family, especially my mother, and my father for their continuous love and support in this journey of life and in any possible manner when I was far away from my parents. I will forever be indebted for their love, patience and wisdom.

Last but not least, I am grateful to my friends whose presence, support and humor have provided an extra boost for me to complete this journey.

CONTENTS

LIST OF FIGURES

LIST OF TABLES

SYMBOLS AND ABBREVIATIONS INDEX

SYMBOL

A_{coll} : collector area (cm^2)

c   : exergy cost per unit ($/GJ)

COP   : coefficient of performance

$\dot{C}$: cost Rate ($/hr)

DNI   : direct normal Irradiations (W/m^2)

$\dot{E}$: energy (kW)

$\dot{EX}$: exergy flows (kW)

f   : exergoeconomic factor (%)

h   : specific enthalpy (kJ/kg)

$\dot{m}$: mass flow rate (kg/s)

n   : system life time

P   : pressure (kPa)

$\dot{Q}$: heat transfer (kW)

s : specific entropy (kJ/kg. K)

T   : temperature (°C)

U   : overall heat transfer coefficient (W/m^2.K)

$\dot{W}$: work done (kW)

Z   : initial cost rate ($/hr)

ŋ   : efficiency (%)

τ   : operation hour (h)

φ : maintenance factor

ψ : exergy efficiency (%)

Abs   : absorber

Coll   : collector

Comp   : compressor

Cond   : condenser

EV	: expansion valve
Evap	: Evaporator
Gen	: generator
SHES	: sensible heat exchanger
SR	: solar reservoir
t	: tank

ABBREVIATION

ARC	: absorption refrigeration cycle
HE	: heat exchanger
HRSG	: heat recovery steam generation
HTF	: heat transfer fluid
ORC	: organic Rankine cycle
ORT	: organic Rankine turbine
P	: pump
PTC	: parabolic trough collectors
RES	: renewable energy sources
SCCHP	: solar combined cooling heating power
SE	: solar energy
TST	: thermal storage tank
VARS	: vapor absorption refrigeration system

PART 1

INTRODUCTION

The global effort to find efficient and sustainable energy solutions has intensified in light of the increasing challenges caused by climate change and the increasing need for energy. Solar-assisted combined Heating, Cooling, and Power (CCHP) system research is a promising avenue to explore in this regard. Innovative solar energy technology meets the diverse energy needs of homes, businesses, and factories with a single, adaptable system. By providing heating, cooling, and electricity generation all in one, these systems provide an all-inclusive answer to the problem of increasing energy use. [1,2].

Renewable energy sources must be integrated in light of the critical need to address climate change. Solar energy can completely transform energy systems since it is both plentiful and ecologically beneficial. Solar-assisted CCHP systems can improve energy efficiency by generating electricity, heating, and cooling all at once. [3–5].

1.1. SOLAR ENERGY

The sun's rays are our planet's most plentiful renewable energy source. It is an eco-friendly and long-lasting energy source derived from the sun's rays. Solar energy (SE) popularity has skyrocketed in recent years because of its many advantages and promising future applications [6].

1.1.1. Benefits of Solar Energy

One significant benefit of solar power is that it doesn't deplete natural resources over time. Solar energy is sustainable since it doesn't depend on finite fossil fuels, which will inevitably deplete over time[7] .

One significant benefit of solar power is that it doesn't deplete natural resources over time. Solar energy is sustainable since it doesn't depend on finite fossil fuels, which will inevitably deplete over time.

Solar power also doesn't contribute to pollution or emissions, making it a green energy option. Because of this, it is a greener option than other energy sources. Because it requires little upkeep, solar power is an economical choice in the long run. The price of solar panels has decreased significantly due to technical breakthroughs and increasing demand, making SE more accessible and affordable for people and companies [6,8].

1.1.2. Applications of Solar Energy

SE has many potential applications, from supplying power for little electronic gadgets to massive manufacturing processes. Some typical applications of solar energy include [9,10]:

- Commercial use: Businesses may reap the benefits of solar energy as well. Indeed, several organizations have begun installing solar panels on their buildings to lower operational expenses and lessen their environmental impact.
- Residential use: A growing number of households opt to put solar panels on their rooftops to produce energy and reduce their dependency on conventional power plants.
- Agriculture: Sustainable and environmentally friendly methods of watering crops are being implemented in agricultural settings via the use of solar-powered irrigation systems and water pumps.
- Street lighting: Solar-powered streetlights, which provide affordable and environmentally friendly lighting options, are gaining popularity in urban areas.
- Transportation: Solar energy is being used for transportation due to the advancement of solar-powered vehicles, including automobiles, buses, and even flights.

- Disaster relief: Solar-powered generators may benefit relief efforts by providing energy during catastrophes or natural disasters.
- Telecommunications: Solar energy is used to power communication towers and equipment in distant places that do not have access to conventional power sources.
- Space exploration: The International Space Station and other spacecraft have been powered by solar energy over their extended missions.

1.1.3. Future of Solar Energy

On the path to a more sustainable future, SE is anticipated to play a pivotal role. Due to research and technology developments, the efficiency and affordable of solar power will increase in the following years [8].

Perovskite solar cells stand out among the most promising new solar energy technologies. Results from these cells have been encouraging, with some research suggesting efficiencies of 30% or more. Because of this, they would outperform conventional solar cells made of silicon in terms of efficiency [11].

Moreover, poorer nations with limited access to conventional power sources have seen a dramatic rise in solar energy use. Many people's lives have been improved because of microgrids and off-grid solar systems that have helped provide energy to rural regions. Furthermore, solar energy integration into commonplace items and infrastructure is rising. Things like road structures with integrated solar panels fall within this category [12].

1.1.4. Parabolic Trough Collectors

Parabolic Trough Collectors (PTCs) are a subset of solar thermal collectors that may gather and convert sunlight into usable heat. They use an illustrative arrangement of long, curved mirrors constructed of reflecting materials to direct sunlight onto a receiving tube. A heat transfer fluid, usually water or oil, is placed in this receiver tube

to collect the concentrated solar energy and transport it for other uses. [13]. Figure 1.1 showed the main components of the PTC collector [14].
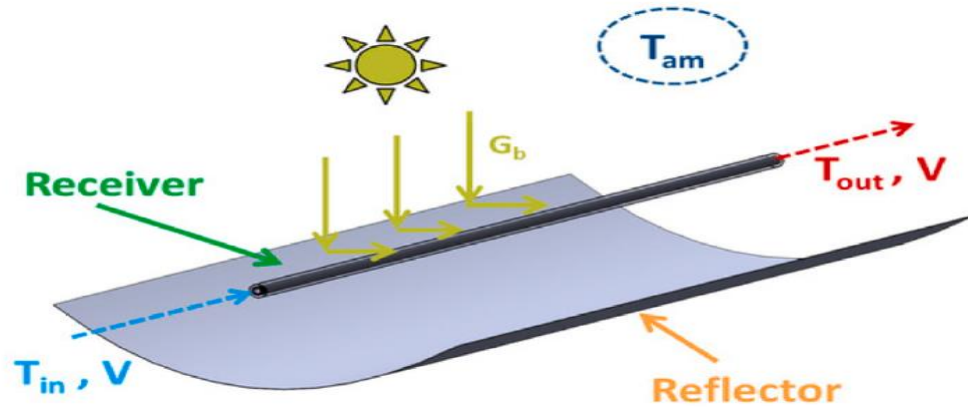
Figure 1.1. Typical parabolic trough collector.

Because they can follow the sun's path all day long, PTCs are much more efficient than other types of solar thermal collectors. The curved mirrors are attached to a tracking system that moves along one axis and tracks the sun's path to catch the most sunlight possible [15].

A key benefit of PTCs is the wide range of applications they may be used for. They have several applications, including home and industrial water heating, powering air conditioning systems, and producing energy via steam turbines [16].

There are environmental advantages to using PTCs in addition to their practical uses. RES do not contribute to air pollution or the release of greenhouse gases, making them eco-friendly. Their long-term viability and little environmental impact make them an ideal energy source.

Famous for its usage in solar thermal technology, PTCs have been in use since the 1980s. They used to be more expensive, but now they're far more efficient and well-designed [13].

1.1.4.1. How do PTCs work?

PTCs include curved mirrors that follow the sun's path throughout the day to make the most of the sun's rays. Next, a receiver tube is positioned at the parabola's focus point to receive the concentrated sunlight. Solar panels collect heat from the sun and transmit it to a fluid within this tube, which may be used to heat water or steam for various purposes. [17].

1.1.4.2. Advantages of PTCs

The efficient conversion of solar energy into heat is one of the primary benefits of PTCs. Mirrors with a parabolic form focus a great deal of sunlight onto a tiny surface, leading to high temperatures and effective energy conversion. PTCs function in both solid and weak sunlight, making them applicable to a wide range of environments [14].

1.1.4.3. Applications of PTCs

Solar thermal power plants employ PTCs to produce energy, which is their most prevalent usage [18]. Industrial activities like desalination and chemical manufacture may also make use of them, as can water heating in homes and businesses. Hybrid solar systems, which combine PTCs with other RES, provide a more stable and environmentally friendly source of electricity. [19].

1.2. ORGANIC RANKINE CYCLE

A thermodynamic cycle known as the Organic Rankine Cycle (ORC) converts heat into mechanical work and produces electricity. Its foundational principles are identical to those of the classic steam Rankine cycle (SRC), with the main exception being that organic fluids, rather than water, serve as the working fluid in an ORC. Because it uses renewable energy sources (RES), including solar, geothermal, and industrial waste heat, it is an environmentally friendly method of producing electricity. [20,21].

1.2.1. Working Principle OF ORC

Similar to the conventional steam SRC, the ORC operates similarly. A heat source, organic fluid, pump, expander, and condenser are the main components of an organic reaction circulation (ORC) system. Once the organic liquid is injected into the heat exchanger, it is heated by the heat source, which might be anything from hot water to exhaust fumes. The expander uses the heated fluid to drive a turbine or another kind of expander, generating mechanical work. After being expanded, the fluid is cooled to a liquid state in the condenser before being sent back to the heat exchanger to start the process. [20].

Organic Rankine Cycles (ORCs) generate mechanical work by vaporizing organic fluids with lower boiling points than conventional steam Rankine Cycles. This means that ORC may be used with heat sources unsuited for use in traditional steam Rankine cycle systems based on higher temperatures.

1.2.2. Applications of ORC

The ORC has a wide range of applications, including [22,23]:

- Integrating ORC systems with solar thermal collectors makes it possible to generate energy using the sun's heat.
- Using subsurface geothermal sources, ORC systems may generate electricity using thermal energy.
- ORC systems may be used in biomass power plants, which heat the cycle by burning organic waste.
- Integrating ORC systems into industrial processes allows for the recovery of waste heat and its subsequent conversion into usable energy, which is known as waste heat recovery.
- Ships seeking a greener and more efficient propulsion system may find ORC (Organic Rankine Cycle) systems to be a viable alternative to steam engines.

Overall, the Organic Rankine Cycle provides a diverse and sustainable solution for various businesses using waste heat and other renewable energy sources. With continued study and development, the possibilities for its uses continue to expand.

1.3. ABSORPTION REFRIGERATION CYCLE

An absorption refrigeration cycle (ARC) is a kind of refrigeration cycle that utilizes heat and other things to produce cooling. This form of refrigeration is widely used in industrial, commercial, and residential settings [24,25].

ARC's four primary parts are an ARC's evaporator, generator, condenser, and absorber. Aside from that, the pump moves the refrigerant around, and the expansion valve regulates its flow [26]. These systems also make use of lithium bromide and water solutions as refrigerants. Figure 1.2 presents the main components of the ARC system.
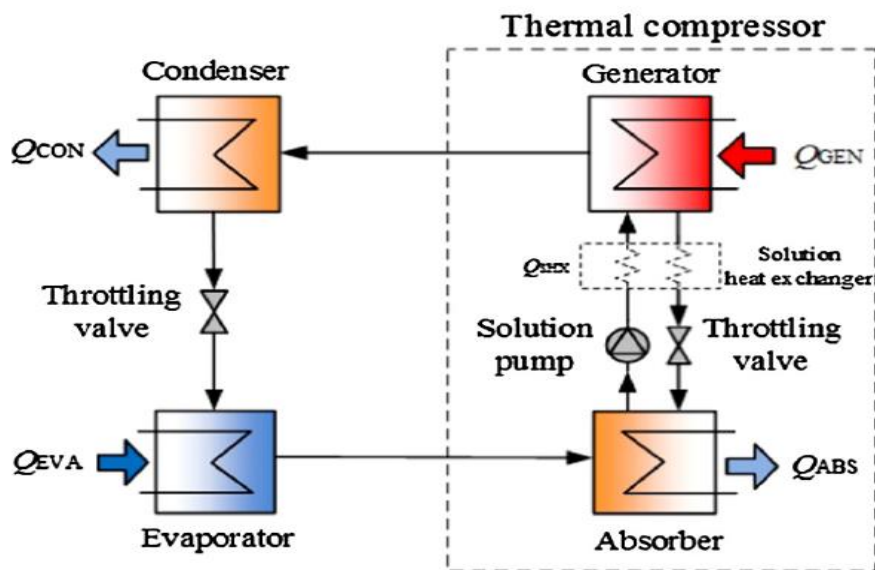
Figure 1.2. Absorption Refrigeration system [27].

1.3.1. Working Principle of ARC

There are three steps in operating an absorption refrigeration system: evaporation, condensation, and absorption. The generator is the first part of the cycle since it is there

that the lithium bromide and water solution is heated. The result is a highly concentrated lithium bromide solution when the water evaporates. Next, it travels to the condenser, which is cooled and transformed into liquid form. The next step is to lower the temperature and pressure of the liquid by passing it through the expansion valve [27].

Next, the cooled refrigerant goes into the evaporator to take up heat from the air and then evaporates again. That vapor is absorbed by the absorber's concentrated lithium bromide solution. A cooling tower or some other method eliminates the heat released during this absorption process. The cycle begins again with the return of the diluted lithium bromide solution to the generator [27].

1.3.2. Applications of ARS

Applications in regions with restricted power supply or rural areas often use absorption refrigeration cycles since energy is not easily accessible in these places. Because they use less energy than conventional compression refrigeration systems, they are trendy in factories that generate a lot of waste heat or steam [28].

Commercial and other large-scale air conditioning systems are typical use case for absorption refrigeration systems. To save energy usage and expenses, these systems may use steam or hot water as a heat source to chill a building.

In addition, food and drink production, chemical processing, and pharmaceutical manufacturing are examples of industrial activities that use absorption refrigeration cycles. They are also common in trailers and vehicles that transport perishable commodities with refrigeration systems.

Many sectors and uses may benefit from the absorption refrigeration cycle since it is a greener and more efficient version of the old compression refrigeration technique. Absorption refrigeration cycles are becoming increasingly attractive for future cooling demands as technology improves efficiency. Therefore, it is not restricted to a specific business or environment but may be used in a wide range of industries and places that

need an effective cooling system. Because they don't utilize ozone-depleting chemicals, absorption refrigeration systems suit the environment and your wallet. This makes it an attractive option for environmentally friendly refrigeration and cooling requirements [29].

1.4. SOLAR-ASSISTED COMBINED COOLING, HEATING AND POWER SYSTEM

An ever-increasing need for more effective energy use has emerged in recent years. Renewable energy sources have recently seen a dramatic increase in use, driven by growing awareness of the need to lessen human impact on the environment. One such source that has grown in popularity is solar power, which is excellent since it is both plentiful and renewable. Solar energy has many potential uses, such as producing electricity, heating and cooling buildings, etc [30].

Innovative and energy-efficient, solar-assisted CCHP uses solar thermal and electricity-generating concepts. Reducing reliance on conventional energy sources, this system uses solar energy to produce power, heat water, and provide air conditioning. Integrating the power generating, heating, and cooling systems into one system is more efficient and cost-effective [31].

Traditionally, cooling, heating, and power generation have been distinct and necessitated using separate systems and energy sources. Nevertheless, technological improvements make it feasible to combine these processes and use a unified system for all three objectives.
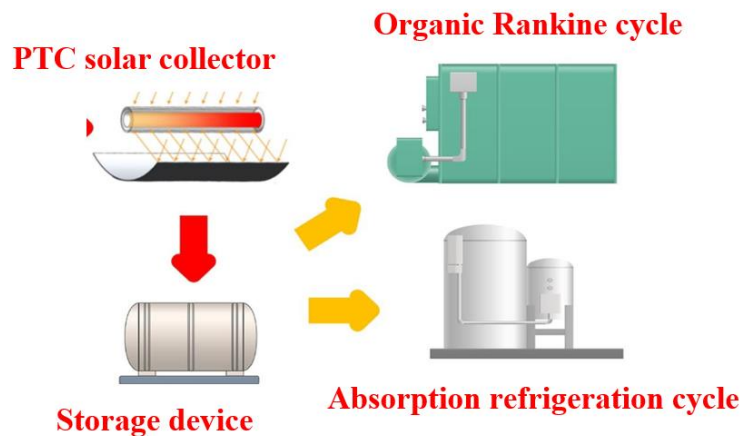
Figure 1.3. Solar-assisted CCHP system.

1.4.1. Benefits of Solar-assisted CCHP

Solar-assisted CCHP systems offer several advantages. First and foremost, they are a renewable energy source that does not produce dangerous compounds or contribute to climate change. Second, using solar power to generate electricity and heat reduces the need for fossil fuels, lowering energy costs. Third, solar-assisted CCHP systems may be tailored to fulfill individual demands and integrated into existing buildings or new projects [32].

1.4.2. Advantages of Solar-assisted CCHP

The advantages of CCHP systems are numerous and wide-ranging. Some of the key benefits include [33]:

- CCHP systems may assist in lowering energy bills for business and residential buildings by using waste heat in conjunction with renewable energy sources.
- In CCHP systems, waste heat generates power and heat and cools the system simultaneously. When compared to typical separate systems, this leads to substantial energy savings.
- When compared to more conventional energy sources, CCHP systems considerably reduce pollution. Because of this, they are a greener choice that may lessen the impact of a structure on the environment.

- In the event of a power outage or other grid disturbance, CCHP systems continue to work constantly, providing a steady energy supply.
- Community combined heat and power (CCHP) systems allow buildings and communities to become more energy-independent, decreasing their need for conventional power plants.
- CCHP systems are adaptable because they may be tailored to fit the demands of a particular structure or neighborhood.

1.5. THESIS MOTIVATION

Research into "Solar-Assisted CCHP Systems" is motivated by the urgent need for sustainable energy solutions and the mounting difficulties caused by climate change. Most of the energy produced by traditional power grids—which rely on fossil fuels—contributes significantly to climate change and other environmental disasters. Incorporating solar energy into a comprehensive system that simultaneously generates electricity, cools, and heats is a game-changer in this regard. The primary motivation for writing this thesis is to find future energy solutions that are less disruptive to nature. One of the key motivators is the pressing need to reduce energy consumption's environmental effect. Utilizing the sun's rays, a limitless and environmentally friendly resource, solar-assisted systems power cooling and heating while also generating electricity. In line with global initiatives to address climate change, these systems provide a way to diversify solar energy use and decarbonize energy production. Research on solar-assisted combined cooling, heating, and power generating systems is underway because of the hope that they may drastically cut down on carbon emissions.

The cost-effectiveness of solar-powered systems is another motivating element. Since the costs and effects of traditional energy sources are difficult to anticipate, we need a viable substitute that won't break the bank. Solar energy has the potential to provide sustainable economic development since it is abundant and becoming cheaper by the day.

In conclusion, the necessity of addressing climate change, improving energy efficiency, and advancing sustainable economic growth serves as the driving force behind this thesis. This study aims to provide essential insights to influence policy choices, direct technical improvements, and facilitate Turkey's transition to a more robust and sustainable energy environment by examining the complexities of Solar-Assisted CCHP Systems.

1.6. THESIS OBJECTIVE

The primary goals of the proposed Solar-assisted CCHP system are listed as:

The primary goals of the proposed Solar-assisted CCHP system are listed as:

- Conducted a simulation analysis of a solar-powered CCHP system in Antalya, Turkey.
- Investigate the effects of various working fluids on the organic Rankine cycle, including R245fa and octane. Evaluate their impact on power production, cooling, and heating output.
- Assess solar energy's impact on CCHP system efficiency and performance under steady-state settings.

PART 2

LITERATURE REVIEW

As the world grapples with rising energy demands and pressing concerns about climate change, the need for sustainable and efficient energy solutions becomes increasingly urgent. In this context, solar-assisted CCHP systems emerge as a beacon of hope. These innovative systems harness the abundant power of the sun to address three critical energy needs simultaneously – a feat impossible with conventional, siloed approaches. This chapter extensively investigates Solar-Assisted CCHP systems, aiming to uncover their possibilities by thoroughly examining existing literature.

Ukaegbu et al. [34] proposed a new approach to improve the overall efficiency of combined CCHP systems by incorporating RES, specifically SE, to complement the thermal input of fossil fuels. The researchers used a multi-objective optimization approach to improve the work net and exergy efficiency while diminishing CO_2 emissions in a solar-assisted CCHP system. The findings demonstrate that a system with substantial work net production does not always lead to a highly efficient system. The research further identified the optimal design characteristics for minimizing CO_2 emissions. The optimization technique produced 100 sets of Pareto optimum solutions, providing decision-makers with a range of options to enhance the efficiency of a solar-assisted CCHP system. The research revealed a contradiction in decision-making processes between CO_2 emission and work net. It found that a higher work net is linked to an undesirable increase in CO2 emissions.

Liu et al. [35] displayed the results of the thermodynamic and exergoeconomic evaluation of a CCHP system driven by a biomass and natural gas co-firing gas turbine combined with a organic Rankine cycle, steam Rankine cycle, and absorption chiller. The findings indicate that the suggested system has a greater energy utilization efficiency, with exergy and thermal efficiencies of 41.76% and 75.69% respectively.

Additionally, the specific utility cost per unit of energy produced is 13.37 $/GJ. The exergy study showed that the combustion chamber is responsible for the majority of the exergy destruction rate.

Gao et al. [36] introduced an innovative cooling-power-desalination combined cycle to use waste heat from shipboard diesel exhaust. This cycle incorporates a freezing desalination sub-cycle to manage the ship's cooling demand changes. A mathematical model was developed to conduct energy and exergy analysis of the cycle to optimize important parameters such as comprehensive efficiency, net output work, and heat exchanger area. The study identified the ideal operating conditions for the system, including the temperature of the generator, seawater, and working fluid composition. Additionally, it performed an economic evaluation of using frozen seawater desalination as a pretreatment for reverse osmosis seawater desalination, which significantly reduced costs. Seeks to address the challenges associated with changes in working circumstances and cooling-load demand in recovering waste heat from diesel exhaust.

Wang et al.[37] suggested a novel integrated power and cooling system using ammonia-water, which enhances the efficiency of utilizing low-temperature heat sources. The system's comprehensive steady-state mathematical model was developed, yielding simulation results for design circumstances. These findings indicate that the thermal efficiency can reach 24.62%, and the exergy efficiency may reach 11.52%. An exergy destruction study revealed that the four heat exchangers and the turbine were the main contributors to the overall exergy destruction. The researchers analyzed the effect of five crucial variables on the system's performance and found that an ideal turbine intake pressure that optimizes the exergy efficiency exists.

Zeng et al. [38] introduced a comprehensive exergoeconomic optimization method for solar absorption-subcooled compression hybrid cooling systems, considering changes in meteorological data and cooling requirements. They developed a comprehensive exergoeconomic model and examined how the size of essential components affects the system's performance. The research examined the differences in ideal sizes based on various weather data. The ideal scenario for the system used in Haikou has a total cost

rate of 13.6% lower than the base case. This suggests that the size of the solar device and compression subsystem is directly proportional to the intensity of local solar radiation and cooling requirements.

Divan et al. [39] suggested a hybrid system connected to an Molten carbonate fuel cell (MCFC) system for combined CCHP applications, capable of synchronizing heating and electricity. The CCHP system can supply cooling and heating loads, with a cooling load of 96 kW and a heating load of 36 kW. The MCFC in the hybrid system produces a total of 117 kW of required power, with 12 kW of power generated for electricity supply. The paper highlights that the hybrid system has the lowest CO_2 emission (4%) and the least pollution. The findings investigated the effect of operating temperature, pressure, and current density parameters on system performance. It reported the hybrid system's overall energy and exergy efficiencies are 54 % and 52.58 %, respectively.

Takleh et al. [40] introduced an efficient solar-geothermal-based system for producing cooling, heating, and power. The study's objective was to evaluate the performance of three working fluids (R1234ze, R423A, and R134yf) by conducting energy, exergy, and thermoeconomic analyses. The study conducted single-objective and multi-objective optimization analyses to maximize thermodynamic and thermoeconomic goals. The results indicated that the R423A working fluid exhibited the lowest rate of total exergy degradation and enhanced energy efficiency compared to the base case's circumstances. Reduction in the levelized cost of heating, cooling, and electricity obtained from multi-objective optimization compared to energy efficiency and cost optimization. The results for R423A working fluid show that Mult objective optimization achieves a levelized cooling, heating, and power cost of 91.17% and 73.22% lower than scenarios optimized solely for energy efficiency and cost considerations. Additionally, the energy efficiency is 13.53 percentage points higher.

Wang et al. [41] introduced a new technique that utilizes emergy-based integrated optimization to enhance the efficiency of hybrid solar building CCHP systems. This method considers the building structures and assesses the system's performance from several perspectives. The evolutionary algorithm is used to determine the optimal characteristics of components in the building's distributed energy system to reduce its yearly energy consumption.

Pokson and Chaiyat [42] developed and implemented a unique prototype for IMW-CCHP. The prototype examined the exergy and energy performance characteristics of the waste-to-energy process, with a focus on the economic implications in terms of the levelized energy cost of the integrated energy system. A cascade connection was established to transfer heat from the incinerator and utilize excess heat from the ORC system for drying and cooling operations. The study demonstrated the advantages of using low-temperature heat at approximately 105°C in the IMW system instead of a geothermal system. The combined system achieved exergy and energy efficiencies of 25.88% and 12.25%, respectively, generating 11.98 kilowatts of three-phase electricity. The chilled water temperature ranged from 10.48 to 11.86 degrees Celsius. When measured in its wet state, the golden longan was dehydrated until it reached a final moisture content of 39.88%. The mean energy cost amounted to 0.136 USD per kilowatt-hour.

Pilou et al. [43] performed research on a comprehensive energy system for office buildings. A numerical tool was used to model systems based on renewable energy. The research primarily examined the renewable energy component of the system, with a particular emphasis on fulfilling the cooling and heating requirements of a standard office building in Athens, Greece, and Copenhagen, Denmark. The research conducted a comparison between technological and environmental indicators and conventional solutions. An important discovery was the significant versatility offered by the heat pump, which could be used to charge the buffer tank. The findings indicated that incorporating conventional PV panels enabled an 82% renewable proportion in Athens and a 61% renewable proportion in Copenhagen for office buildings with intermediate energy efficiency standards.

Zisopoulos et al. [44] introduced a novel thermal system called MiniStor incorporating thermochemical heat storage (TCM) technology. This novel method employed the $CaCl_2/NH_3$ cycle, a reversible reaction involving an ammoniated calcium chloride salt and ammonia, to generate heating and cooling effects. The system aims to harness RES, particularly solar energy, for sustainable power. An integrated thermal system thermodynamic model was developed using Matlab/Simulink and Aspen Plus Dynamics to evaluate the system's performance and characteristics. The simulations

revealed that the system can adequately fulfill the building's heat demands, achieving an average maximum efficiency of 93% and a minimum efficiency of 81% during winter. Furthermore, the system exhibited a modest cooling capacity of 34% during summer. The coefficient of performance (COP) for heating and cooling was determined to be 1.71 and 0.47, respectively, resulting in an overall system efficiency of 128% for heating and 41% for cooling.

Al-Sayyab et al. [45] introduced a new waste heat-solar driven ejector-compression heat pump that utilizes low global warming alternative refrigerants instead of R134a. They investigated various system configurations to improve the coefficient of performance (COP) under overcast day conditions. The study used real weather data from three European cities to assess the theoretical performance of the proposed system. The cooling COP and carbon dioxide emission reductions of alternative refrigerants (R513A and R450A) and R134a were compared. The simulations demonstrated that using R450A could improve the cooling COP by 7% compared to a conventional R134a vapor compression system. The heating mode showed the most significant increase in COP, with waste heat and the use of R450A resulting in a COP increase of up to 75.0% compared to the baseline scenario using R134a. Based on the highest equivalent CO_2 emission reduction, the study recommends the proposed R450A systems from an environmental perspective.

Yan et al. [46] proposed a method for optimizing the capacity of a hybrid CCHP system integrated with geothermal, solar, and wind energy. The method considers environmental impact, energy supply independence, energy efficiency, and economic performance. The researchers used a stochastic hierarchy scenario-generation method to account for uncertainties in multiple loads, solar irradiation, and wind velocity. The research assessed the hybrid system's adaptability in terms of its integration with the power grid and its interaction with the net. The environmental performance assessment was conducted by evaluating the rate of carbon emission reduction and the level of renewable energy integration. Meanwhile, the economic performance evaluation was based on the yearly cost-saving rate, while the energy performance assessment focused on the primary cost-saving rate.

Ao et al. [47] introduced a multi-objective stochastic multi-scenario optimization technique to enhance the capacity of a hybrid CCHP model. The flexibility of the hybrid system was evaluated based on the net interaction level and grid integration level. The environmental performance was evaluated by calculating the rate of lowering CO_2 emissions and the level of renewable energy integration. In contrast, the economic and energy performances were distinguished by their yearly and main cost-saving rates, respectively. The authors also formulated and solved the multi-objective stochastic optimal design method using the non-dominated sorting genetic algorithm II. The findings demonstrated that the proposed stochastic multi-scenario optimization method saves computation time compared to traditional optimizations and provides insights into the impact of increasing the installed capacity of electrical energy storage and renewable energy generators on system performance.

Wang et al. [48] introduced a novel approach to improve the efficiency of SE utilization by integrating a CCHP system with a full-spectrum hybrid SE device. This device comprises molecular solar thermal (MOST) and water heating (SWH) systems. The integration of the CCHP system with MOST system and SWH system, for the first time, allows for the utilization of the entire solar energy spectrum. The CCHP system, powered by SE and methanol, operates independently of external conditions, making it suitable for cloudy days and at night. The study presents thermodynamic models of the system components, evaluation indicators, and simulation results under design conditions. The findings demonstrate that the proposed system achieves a solar energy share of 45.07% and exergy and energy efficiencies of 26.59% and 70.65% in cooling mode, respectively. Furthermore, compared to a conventional methanol direct-fired system, the proposed system achieves primary energy savings and CO_2 emission reductions of 16.20% and 16.14%, respectively.

Nami et al. [49] proposed a solar-assisted biomass-based trigeneration system for meeting domestic energy needs. The system was analyzed from both thermodynamics and sustainability perspectives. The researchers examined the key components of the integrated system to identify the units that consume the most exergy. They also investigated how various decision parameters and seasonal conditions affect the system's performance. The simulation results demonstrated that the proposed system

can provide space heating, domestic hot water, chilled water for cooling, and 1MW power. Furthermore, the research determined that the air compressor's pressure ratio, the gas turbine's intake temperature, and the temperature differential inside the air heater are essential criteria for maximizing the system's performance.

Cavalcanti et al. [50] developed a thermal performance model for evacuated tube solar collectors, incorporating the global irradiation parameter and collector loops. The authors also constructed a model for a mixed-effect absorption chiller, considering increased engine capacity and enhanced separation process for the non-ideal LiBr mixture. They then compared their developed model to existing literature data. The findings confirmed the impact of dead state temperature on the exergy efficiency of the components in an ARC that utilized a mixture of H_2O and LiBr.

Wang et al. [51] suggested a stochastic optimization model for a hybrid CCHP system that takes into account uncertainties in load demands and renewable energy sources (RES). Considering their off-design characteristics, they developed energy hub models for storage devices and energy converters. The simulation used the non-dominated sorting genetic algorithm II to enhance the hybrid CCHP system. The method considered system dependability and aimed to attain optimal energetical, economic, and environmental advantages. A case study has shown that decreased system dependability results in a reduction of greenhouse gas emissions and more excellent energy-saving advantages.

Wang et al. [52] introduced a new hybrid CCHP system that combines solar thermal biomass gasification and effectively utilizes both solar energy and biomass. The research sought to mitigate the volatility and intermittency of solar energy by integrating biomass into the hybrid CCHP system. The study investigated the thermodynamic performances of the hybrid CCHP system, using exergy and energy efficiency as assessment metrics. It also analyzed the effects of electric solar irradiance and load ratio on the CCHP system and discussed the advantages of biomass gasification with the assistance of SE. The simulation demonstrated that the CCHP system attained mean exergy and energy efficiencies of 28% and 56%, respectively. During full-load operation, the energy ratio between sun and biomass is around 0.19.

The use of SE in the biomass gasification CCHP system resulted in a 55.09% increase in the heating value of the produced gas, compared to the traditional system that does not employ SE. Furthermore, the suggested hybrid system decreased the use of biomass by about 2.02% and 9.22% in the heating and cooling modes, respectively. The data unequivocally showed that the suggested hybrid system significantly and practically improved the efficiency of using biomass energy.

Saini et al. [53] proposed a new solar-driven CCHP system for small buildings in remote areas. The system combines various components, including thermal energy storage, evacuated tube collectors, ejector refrigeration cycle, water heater, and organic Rankine cycle, to generate power, heating, and cooling. The study evaluated different factors, such as cooling cost, exergy efficiency, power cost, total cost per output, heating cost, and equivalent CO_2 emission. Parametric studies were conducted to observe how decision variables, such as evaporator temperature, generator temperature, pinch point temperature difference, condenser temperature, and turbine mass fraction, influenced these factors. The findings indicated that increasing evaporator or generator temperature improved CO2 emission, exergy efficiency, and heating cost while reducing power and cooling costs. On the other hand, rising condenser temperature diminishes power and cooling costs, and exergy efficiency, while increasing CO2 emissions and heating cost. Additionally, increasing turbine mass fraction improved exergy efficiency, CO2 emission, and power cost while reducing cooling and cooling-power cost ratios. Overall, the offered CCHP system appears suitable for meeting future energy demands regarding cooling, heating, and power production.

Ramos et al. [54] investigated the feasibility and cost-effectiveness of hybrid photovoltaic-thermal (PV-T) systems for generating energy in residential buildings. The study focused on ten different locations in Europe and examined the potential of PV-T systems to meet a significant portion of household heating and cooling needs. Integrating PV-T panels with water-to-water heat pumps achieved an optimal system design. The research used precise system performance estimates derived from hourly resolved transient models in TRNSYS, considering the temporal resolution of simulations. The findings demonstrated that PV-T systems can fulfill a significant

proportion of the cooling and heating requirements in residential properties at the investigated sites. Moreover, the total energy expenditure for PV-T systems was 30-40% less than PV-only systems of the same capacity, making them economically appealing.

Fani and Sadreddin [33] proposed a system configuration for office buildings in Iran that combines solar power with cooling, heating, and power (CCHP). This configuration includes a heat storage tank and both compression and absorption chillers connected to the conventional system. The study conducted an hourly simulation using real conditions from a case study. It analyzed the energy balance, production strategies, and economic feasibility of the solar-assisted CCHP system. The study examined four operational strategies for the CCHP system: following thermal load (FTL), hybrid supply for cooling demand, following electrical load (FEL), and an optimization model. It also assessed the optimal equipment size and the reduction in CO_2 emissions. The findings highlighted the solar-assisted CCHP system's superior efficiency, cost benefits, and greenhouse gas emission reduction. The results indicated that the overall system efficiency can reach up to 89% in summer, with a potential reduction of 2217 kg/day in CO_2 emissions during winter.

PART 3

SOLAR-ASSISTED CCHP SYSTEM MODELLING

3.1. MODEL DESCRIPTION

Solar-assisted CCHP systems are hybrid energy systems that simultaneously utilize solar energy to produce electricity, heating, and cooling. The Solar-assisted CCHP system consists of several components, including solar collectors, an organic Rankine cycle (ORC) unit, absorption chiller, and thermal energy storage, as shown in Figure 3.1. Each component plays a crucial role in the overall functioning of the system.

The solar collectors are responsible for capturing and converting solar energy into thermal energy. The type of solar collector that is used in this model is parabolic solar collectors. The concentrated sunlight is directed onto a receiver tube at the parabola's focal point. This tube contains Therminol 66 as a heat transfer fluid, which is heated by intense solar energy and then circulated through a thermal storage tank (TST) to store superheated steam. The Therminol 66, held in the TST, is circulated through the evaporator of the ORC to produce superheated steam.

The ORC, also referred to as a cogeneration unit, simultaneously generates electricity and thermal energy. It achieves this by utilizing the waste heat from power generation for heating purposes via the condenser. As a result, it offers higher overall efficiency compared to conventional systems that separately generate electricity and provide heating or cooling.

 The exhaust heat generated from the evaporator of the ORC is used to drive the absorption chiller. The absorption chiller is responsible for converting thermal energy into cooling power. It uses a solution of lithium bromide and water to absorb heat from

the building or process it is cooling, resulting in chilled water that can be circulated throughout the system.

Thermal energy storage allows the storage of excess thermal energy produced by the system during periods of low demand. This stored energy can then be used during peak demand times, increasing the overall efficiency and reliability of the system.

The following assumptions are employed in the modelling of the system:

- The system and its components are in a state of steady state.
- The solar energy component utilizes Therminol-66 oil as the chosen working fluid to efficiently transmit heat from the solar collectors to the storage tank, ARS generator, and ORC evaporator.
- The LiBr- H_2O solutions leaving the generator is in a saturated state.
- The refrigerant steam leaving the evaporator and the refrigerant liquid leaving the condenser are both in a saturated state.
- The throttling valve operates under isenthalpic conditions.
- The effectiveness of the SHEX is 0.7.
- There are no pressure losses accounted for in the pipes and heat exchangers.

Figure 3.1. Schematic diagram for Solar-assisted CCHP system .

Table 3.1. Input data for modeling of the suggested SCCHP.

Parameter	Value
Solar area (m^2)	510130 m^2
Sun temperature	5770 K
Solar reservoir outlet temperature	243° C
Solar reservoir inlet temperature	127° C
Latitude (N)	36.54° N
Longitude (E)	30.41° E
Location	Antalya, Turkey
Direct normal irradiation (DNI)	6.25 kWh/ m^2.day
T$_{amb}$	25° C
P$_{amb}$	101kPa
Compressor inlet pressure (P$_{25}$)	400 kPa
Compressor exit pressure (P$_{22}$)	1200 kPa
Absorber temperature (T$_{12}$)	36° C
Cascade condenser exit temperature (T$_{21}$)	6.3° C
Generator temperature (T$_{15}$)	90° C
LiBr solution strength	55%
Compressor efficiency	85%
ORC turbine efficiency	90%
ORC pump efficiency	80%

3.2. THERMODYNAMIC ANALYSIS

3.2.1. Mass Balance

The concept of mass conservation is a key tenet in all thermodynamic analyses, and it is defined as follows:

$$\sum \dot{m}_{in} - \sum \dot{m}_{out} = \frac{dm_{cv}}{dt} \tag{3.1}$$

Here, $\dot{m}$ represents the rate at which mass flows, and cv represents the control volume. Additionally, the symbols in and out denote the entrance and exit points of the control volume.

3.2.2. Energy Balance

The energy balance equation of a control volume pertains to the total energy entering and leaving via all inlets and outlets. The first law of thermodynamics, known as the law of energy conservation, may be represented as [55,56]:

$$\dot{Q} - \dot{W} + \sum \dot{E}_{in} - \sum \dot{E}_{out} = \frac{dE_{cv}}{dt} \qquad (3.2)$$

The CCHP system's energy and mass balance equations are shown in Table 3.2.

Table 3.2. The CCHP system's energy and mass balance equations.

Component	equation
PTC	$\dot{Q}_{Solar} = A_{Coll}.DNI.N_{Coll}$ $\dot{Q}_{Solar,\,in} = \dot{Q}_{Solar}.\eta_{coll} = \dot{m}_{20}(h_{20} - h_{31})$
Pump 4	$\dot{W}_{Pump\,4} = \dot{m}_{19}(h_{31} - h_{19})$
TES	$\dot{Q}_{St} = \dot{Q}_{TST,in} - \dot{Q}_{Loss} - \dot{Q}_{ORC,Evap}$ $\dot{Q}_{St} = \rho.V.C_p.\frac{dT_{st}}{dt}$ $\dot{Q}_{TST,in} = \dot{m}_{20}(h_{20} - h_{19})$ $\dot{Q}_{loss} = A_t.u_t.(T_{st} - T_{amb})$
Pump 1	$\dot{W}_{Pump\,2} = \dot{m}_{17}(h_{18} - h_{17})$
ORC boiler	$\dot{Q}_{ORC,Evap} = \dot{m}_{21}(h_{21} - h_{22}) = \dot{m}_1(h_1 - h_6)$
ORT	$\dot{W}_{ORT} = \dot{m}_1(h_1 - h_2)$
Regenerator	$\dot{Q}_{Reg} = \dot{m}_2(h_2 - h_3) = \dot{m}_5(h_5 - h_6)$
Condenser	$\dot{m}_3(h_3 - h_4) = \dot{m}_{23}(h_{24} - h_{23})$
Pump 2	$\dot{W}_{Pump\,2} = \dot{m}_4(h_5 - h_4)$
Generator	$\dot{m}_{22}(h_{22} - h_{17}) = \dot{m}_{10}h_{10} - \dot{m}_9h_9 + \dot{m}_9h_9$
SHEX	$\dot{m}_9(h_9 - h_8) = \dot{m}_{10}(h_{10} - h_{11})$
Absorber	$\dot{m}_{29}(h_{30} - h_{29}) = \dot{m}_{12}h_{12} - \dot{m}_7h_7 + \dot{m}_{16}h_{16}$
Pump 4	$\dot{W}_{Pump\,4} = \dot{m}_7(h_8 - h_7)$
EV2	$h_{11} = h_{12}$
Condenser 2	$\dot{m}_{13}(h_{13} - h_{14}) = \dot{m}_{25}(h_{26} - h_{25})$
EV1	$h_{14} = h_{15}$
Evaporator	$\dot{Q}_{Evap} = \dot{m}_{15}(h_{16} - h_{15}) = \dot{m}_{27}(h_{27} - h_{28})$

3.2.3. Entropy Balance

The amount of entropy produced in a system is directly related to the losses occurring in that system, and it is defined as follows [57,58]:

$$\dot{S}_{gen} = \sum \dot{m}_{out} s_{out} - \sum \dot{m}_{in} s_{in} - \sum \frac{\dot{Q}}{T_K} + \frac{ds_{cv}}{dt} \tag{3.3}$$

Here, T_K and $\dot{Q}$ represent the temperature of the heat source and the heat transfer from the fluid supply, respectively. The CCHP system's entropy generation equations for each component are illustrated in Table 3.3.

Table 3.3. The CCHP system's entropy generation equations

Component	equation
PTC	$\dot{S}_{gen,PTC} = \dot{m}_{20}(s_{20} - s_{31}) - \frac{\dot{Q}_{Solar,\,in}}{T_{sun}}$
Pump 4	$\dot{S}_{gen,P4} = \dot{m}_{19}(s_{31} - s_{19})$
TES	$\dot{S}_{gen,TST} = \dot{m}_{18}(s_{21} - s_{18}) - \dot{m}_{20}(s_{20} - s_{19})$
Pump 1	$\dot{S}_{gen,P1} = \dot{m}_{17}(s_{18} - s_{17})$
ORC boiler	$\dot{S}_{gen,ORC,Evap} = \dot{m}_{21}(s_{21} - s_{22}) - \dot{m}_1(s_1 - s_6)$
ORT	$\dot{S}_{gen,ORT} = \dot{m}_1(s_1 - s_2)$
Regenerator	$\dot{S}_{gen,Reg} = \dot{m}_2(s_2 - s_3) - \dot{m}_5(s_5 - s_6)$
Condenser	$\dot{S}_{gen,Con} = \dot{m}_3(s_3 - s_4) - \dot{m}_{23}(s_{24} - s_{23})$
Pump 2	$\dot{S}_{gen,P2} = \dot{m}_4(s_5 - s_4)$
Generator	$\dot{S}_{gen,Gen} = \dot{m}_{22}(s_{22} - s_{17}) - \dot{m}_{10}s_{10} - \dot{m}_9 s_9 + \dot{m}_9 s_9$
SHEX	$\dot{S}_{gen,SHEX} = \dot{m}_{10}(s_{10} - s_{11}) - \dot{m}_9(s_9 - s_8)$
Absorber	$\dot{S}_{gen,abs} = \dot{m}_{12}s_{12} - \dot{m}_7 s_7 + \dot{m}_{16}s_{16} - \dot{m}_{29}(s_{30} - s_{29})$
Pump 4	$\dot{S}_{gen,P4} = \dot{m}_7(s_8 - s_7)$
EV2	$\dot{S}_{gen,EV2} = s_{11} - s_{12}$
Condenser 2	$\dot{S}_{gen,Con} = \dot{m}_{13}(s_{13} - s_{14}) - \dot{m}_{25}(s_{26} - s_{25})$
EV1	$\dot{S}_{gen,EV2} = s_{14} - s_{15}$
Evaporator	$\dot{S}_{gen,Evap} = \dot{m}_{27}(s_{27} - s_{28}) - \dot{m}_{15}(s_{16} - s_{15})$

3.3. EXERGY ANALYSIS

3.3.1. Exergy Destruction

The fundamental objectives in exergy analysis of a system are often focused on the destruction and loss of energy. Since these processes are the main contributors to inefficiencies in heat-chemical systems, research is being conducted to examine and suggest strategies to decrease these losses. The exergy balance for a steady-state system is defined as follows[59] :

$$\dot{Ex}_{in} + \dot{Ex}_Q = \dot{Ex}_{out} + \dot{Ex}_W + \dot{Ex}_{dis} \tag{3.4}$$

Here, $\dot{Ex}_Q$ represents the exergy rate associated with the transmission of heat, $\dot{Ex}_{out}$ symbolizes the exergy flow rate at the exit, whereas $\dot{Ex}_{in}$ represents the exergy flow rate at the entrance. Besides, the variable $\dot{Ex}_W$ represents the rate at which work is transferred, with a positive value indicating work done by the system, and $\dot{Ex}_{dis}$ is the exergy destruction rate. For each term in Eq. ((3.4), we have the corresponding equations [60–62]:

$$\dot{Ex}_{in} = \dot{m}ex_{in} \tag{3.5}$$

$$\dot{Ex}_{out} = \dot{m}ex_{out} \tag{3.6}$$

$$\dot{Ex}_Q = \dot{Q}_i \left(1 - \frac{T_0}{T_i} \right) \tag{3.7}$$

$$\dot{Ex}_W = \dot{W} \tag{3.8}$$

$$\dot{Ex}_{dis} = T_0 \dot{s}_{gen} \tag{3.9}$$

where T_0 and $\dot{s}_{gen}$ represent the dead-state temperature and entropy production resulting from irreversibility in the system.

3.3.2. Exergy Efficiency

The exergy product refers to the valuable flow of exergy generated by a system or component, which is directly linked to the thermodynamic output of the component. Thus, the exergy efficiency of a system is determined by characterizing the fuel and product of the component based on the exergy idea of surplus efficiency [59].

$$\eta_{ex} = \frac{\dot{Ex}_p}{\dot{Ex}_f} = 1 - \frac{\dot{Ex}_{des}}{\dot{Ex}_f} \tag{3.10}$$

$\dot{\mathrm{E}}\mathrm{x}_p$ represents the exergy flow of the product, whereas $\dot{\mathrm{E}}\mathrm{x}_f$ represents the exergy flow of the fuel in the system. Fuel and product exergies in different components of the CCHP system are presented in Table 3.4.

Table 3.4. Fuel and product exergies in different components of the CCHP system.

Component	$\dot{\mathbf{E}}\mathbf{x}_f$	$\dot{\mathbf{E}}\mathbf{x}_p$
PTC	$\dot{Q}_{solar}\left(1-\frac{T_0}{T_{sun}}\right)$	$\left(\dot{\mathrm{E}}\mathrm{x}_{20}-\dot{\mathrm{E}}\mathrm{x}_{31}\right)$
Pump 4	$\dot{W}_{Pump\,4}$	$\dot{\mathrm{E}}\mathrm{x}_{31}-\dot{\mathrm{E}}\mathrm{x}_{19}$
TES	$\dot{\mathrm{E}}\mathrm{x}_{20}-\dot{\mathrm{E}}\mathrm{x}_{19}$	$\dot{\mathrm{E}}\mathrm{x}_{21}-\dot{\mathrm{E}}\mathrm{x}_{18}$
Pump 1	$\dot{W}_{Pump\,1}$	$\dot{\mathrm{E}}\mathrm{x}_{18}-\dot{\mathrm{E}}\mathrm{x}_{17}$
ORC Evaporator	$\dot{\mathrm{E}}\mathrm{x}_{21}-\dot{\mathrm{E}}\mathrm{x}_{22}$	$\dot{\mathrm{E}}\mathrm{x}_{1}-\dot{\mathrm{E}}\mathrm{x}_{6}$
ORT	$\dot{\mathrm{E}}\mathrm{x}_{1}-\dot{\mathrm{E}}\mathrm{x}_{2}$	$\dot{W}_{OTR}$
Regenerator	$\dot{\mathrm{E}}\mathrm{x}_{2}-\dot{\mathrm{E}}\mathrm{x}_{3}$	$\dot{\mathrm{E}}\mathrm{x}_{6}-\dot{\mathrm{E}}\mathrm{x}_{5}$
Condenser	$\dot{\mathrm{E}}\mathrm{x}_{3}-\dot{\mathrm{E}}\mathrm{x}_{4}$	$\dot{\mathrm{E}}\mathrm{x}_{24}-\dot{\mathrm{E}}\mathrm{x}_{23}$
Pump 2	$\dot{W}_{Pump\,2}$	$\dot{\mathrm{E}}\mathrm{x}_{5}-\dot{\mathrm{E}}\mathrm{x}_{4}$
Generator	$\dot{\mathrm{E}}\mathrm{x}_{22}-\dot{\mathrm{E}}\mathrm{x}_{17}$	$\dot{\mathrm{E}}\mathrm{x}_{10}-\dot{\mathrm{E}}\mathrm{x}_{9}+\dot{\mathrm{E}}\mathrm{x}_{13}$
SHEX	$\dot{\mathrm{E}}\mathrm{x}_{10}-\dot{\mathrm{E}}\mathrm{x}_{11}$	$\dot{\mathrm{E}}\mathrm{x}_{9}-\dot{\mathrm{E}}\mathrm{x}_{8}$
Absorber	$\dot{\mathrm{E}}\mathrm{x}_{16}-\dot{\mathrm{E}}\mathrm{x}_{7}+\dot{\mathrm{E}}\mathrm{x}_{12}$	$\dot{\mathrm{E}}\mathrm{x}_{30}-\dot{\mathrm{E}}\mathrm{x}_{29}$
Pump 4	$\dot{W}_{Pump\,4}$	$\dot{\mathrm{E}}\mathrm{x}_{8}-\dot{\mathrm{E}}\mathrm{x}_{7}$
EV2	$\dot{\mathrm{E}}\mathrm{x}_{11}$	$\dot{\mathrm{E}}\mathrm{x}_{12}$
Condenser 2	$\dot{\mathrm{E}}\mathrm{x}_{13}-\dot{\mathrm{E}}\mathrm{x}_{14}$	$\dot{\mathrm{E}}\mathrm{x}_{26}-\dot{\mathrm{E}}\mathrm{x}_{25}$
EV1	$\dot{\mathrm{E}}\mathrm{x}_{14}$	$\dot{\mathrm{E}}\mathrm{x}_{15}$
Evaporator	$\dot{\mathrm{E}}\mathrm{x}_{27}-\dot{\mathrm{E}}\mathrm{x}_{28}$	$\dot{\mathrm{E}}\mathrm{x}_{16}-\dot{\mathrm{E}}\mathrm{x}_{15}$

3.4. EXERGOECONOMIC ANALYSIS

3.4.1. Exergy Pricing

The exergy cost mechanism assigns a cost to each exergy flow, and the cost rate associated with the ith flow is denoted as C and given by Eq. (3.10) [63,64].

$$\dot{C}_i = c_i \dot{\mathrm{E}}\mathrm{x}_i \tag{3.11}$$

where c_i represents the cost per unit of exergy (\$/kW.hr) and $\dot{\mathrm{Ex}}_i$ represents the rate at which exergy flows. Furthermore, a cost is assigned to the exergy flow that corresponds to the transmission of heat and work.

$$\dot{C}_Q = c_q \dot{\mathrm{Ex}}_q = c_q \dot{Q}_q \left(1 - \frac{T_0}{T_q}\right) \tag{3.12}$$

$$\dot{C}_W = c_w \dot{W} \tag{3.13}$$

3.4.2. Cost Balance

The following equation represents the overall balance for component cost analysis [65,66]:

$$\Sigma \left(c_{in}\dot{\mathrm{Ex}}_{in}\right)_k + c_{q,k}\dot{\mathrm{Ex}}_{q,k} + \dot{Z}_k = \Sigma \left(c_{out}\dot{\mathrm{Ex}}_{out}\right)_k + c_{w,k}\dot{W}_k \tag{3.14}$$

The cost rate for the kth component, denoted as $\dot{Z}_k$, and it is calculated as follows [26,67]:

$$\dot{Z}_k = z_k * CRF * \frac{\phi}{N} \tag{3.15}$$

$$CRF = \frac{i(1+i)^N}{(1-i)^N - 1} \tag{3.16}$$

Where the variable z_k represents the initial purchase cost of the component, φ represents the coefficient associated with the component's repair and maintenance cost, N represents the number of hours the component performs annually, and i and n indicate the capital profit rate and the year of system performance, respectively. CRF stands for capital recovery factor. The initial purchase cost of the different components of the CCHP system are presented in Table 3.5.

Table 3.5. The CCHP system's entropy generation equations.

Component	Equation	Reference
PTC	$\dot{Z}_{SPTC} = 126.\,A_c$	[68]
Pump	$\dot{Z}_P = 3450\,\dot{W}_{pump}{}^{0.71}$	[69]
TES	$\dot{Z}_{TST} = 1380.\,V_{TST}{}^{0.4\,0.4}$	[70]
Evaporator	$\dot{Z}_{,Evap} = 235.\,\dot{Q}_{Evap}$	[68]
ORT	$\dot{Z}_{ORT}$ $= (479.34 \times \dot{m}_7/0.92 - \eta_T)Ln(p_1/p_2)\,\big(1$ $+ \exp(0.036 \times T_1 - 54.4)\big)$	[71]
Regenerator	$\dot{Z}_{Reg} = 235.\,\dot{Q}_{Reg}$	[72]
Condenser	$\dot{Z}_{cond} = 1173.\,\dot{m}_{fluid}$	[73]
Generator	$\dot{Z}_{Gen} = 190 + 130\,A_{Gen}$	[69]
SHEX	$\dot{Z}_{SHEX} = 190 + 130\,A_{SHEX}{}^{0.85}$	[69]
Absorber	$\dot{Z}_{Abs} = 190 + 130\,A_{Abs}$	[69]
Expansion valve	$\dot{Z}_{EV1} = 114.5.\,\dot{m}_{fluid}$	[69]

The key parameters for the exergoeconomic evaluation of the system are shown in Table 3.4. Table 3.5 includes the cost balances and auxiliary equations for each system component.

Table 3.6. Exergoeconomic evaluation parameters of GT–HRSG/ORC [74].

Main costs per exergy unit of fuel	$c_{F,k} = \dfrac{\dot{C}_{F,k}}{\dot{E}_{F,k}}$
Main costs per exergy unit of product	$c_{P,k} = \dfrac{\dot{C}_{P,k}}{\dot{E}_{P,k}}$
Cost rate of exergy destruction	$\dot{C}_{D,k} = c_{F,k}\dot{E}_{D,k}$
Exergoeconomic factor	$f_k = \dfrac{\dot{Z}_k}{\dot{Z}_k + \dot{C}_{D,k}}$

Table 3.7. Cost analysis OF THE CCHP system.

Components	Cost equation	Auxiliary Equations
ORT	$\dot{C}_1 + \dot{Z}_{ORT} = \dot{C}_2 + \dot{C}_{ORT}$	$c_1 = c_2$
Regenerator	$\dot{C}_2 + \dot{C}_5 + \dot{Z}_{Reg} = \dot{C}_3 + \dot{C}_6$	$c_2 = c_3$
Condenser	$\dot{C}_3 + \dot{C}_{23} + \dot{Z}_{cond1} = \dot{C}_{24} + \dot{C}_{27}$	$c_3 = c_4$
Pump 2	$\dot{C}_4 + \dot{Z}_{P2} = \dot{C}_5$	$c_{ORT} = c_{P1}$
Boiler	$\dot{C}_{21} + \dot{C}_6 + \dot{Z}_{Boiler} = \dot{C}_1 + \dot{C}_{22} + \dot{C}_{Boiler}$	$\dfrac{\dot{C}_{21}}{\dot{EX}_{21}} = \dfrac{\dot{C}_{22}}{\dot{EX}_{22}}$
Generator	$\dot{C}_{22} + \dot{C}_9 + \dot{Z}_{Gen} = \dot{C}_{17} + \dot{C}_{10} + \dot{C}_{13}$	$\dfrac{\dot{C}_{10} - \dot{C}_9}{\dot{EX}_{10} - \dot{EX}_9} = \dfrac{\dot{C}_{13} - \dot{C}_9}{\dot{EX}_{13} - \dot{EX}_9}$
SHEX	$\dot{C}_8 + \dot{C}_{10} + \dot{Z}_{SHEX} = \dot{C}_{11} + \dot{C}_9$	$c_{10} = c_{11}$
Pump 3	$\dot{C}_7 + \dot{Z}_{P3} = \dot{C}_8$	
PRV	$\dot{C}_{11} + \dot{Z}_{PRV} = \dot{C}_{12}$	
Absorber	$\dot{C}_{16} + \dot{C}_{12} + \dot{C}_{29} + \dot{Z}_{Abs} = \dot{C}_7 + \dot{C}_{30}$	$\dfrac{\dot{C}_7}{\dot{EX}_7} = \dfrac{\dot{C}_{12} + \dot{C}_{16}}{\dot{EX}_{12} + \dot{EX}_{16}}$
Evaporator	$\dot{C}_{15} + \dot{C}_{27} + \dot{Z}_{Evap} = \dot{C}_{16} + \dot{C}_{28}$	$c_{15} = c_{16}$
Expansion Valve	$\dot{C}_{14} + \dot{Z}_{EV} = \dot{C}_{15}$	
Condenser 2	$\dot{C}_{13} + \dot{C}_{25} + \dot{Z}_{Cond2} = \dot{C}_{14} + \dot{C}_{26}$	$c_{13} = c_{14}$
PTC	$\dot{C}_{31} + \dot{Z}_{PTC} = \dot{C}_{21}$	
Pump 4	$\dot{C}_{19} + \dot{Z}_{P4} = \dot{C}_{31}$	
TST	$\dot{C}_{20} + \dot{C}_{18} + \dot{Z}_{TST} = \dot{C}_{21} + \dot{C}_{19} + \dot{C}_{TST}$	$c_1 = c_2$
Pump 1	$\dot{C}_{17} + \dot{Z}_{P1} = \dot{C}_{18}$	

3.5. OUTPUT PERFORMANCE PARAMETERS

Lastly, the following indicators are added to examine the performance of the CCHP system:

Overall output work:

$$\dot{W}_{net} = \dot{W}_{ORT} - \dot{W}_{P1} - \dot{W}_{P2} - \dot{W}_{P3} - \dot{W}_{P4} \tag{3.17}$$

Overall efficiency:

$$\eta_{\text{CCHP}} = \frac{\dot{W}_{net} + \dot{Q}_{heating} + \dot{Q}_{cooling}}{A_{Coll}.\eta_{coll}.DNI.N_{Coll}} \qquad (3.18)$$

$$\psi_{\text{SCCHP}} = \frac{\dot{W}_{net} + \dot{EX}_{P,heating} + \dot{EX}_{P,cooling}}{\dot{Q}_{solar}\left(1 - \frac{T_0}{T_{sun}}\right)} \qquad (3.19)$$

Coefficient of performance

$$\text{COP}_{\text{VARS}} = \frac{\dot{Q}_{Evaporator}}{\dot{Q}_{Generator} + \dot{W}_{Pump\ 3}} \qquad (3.20)$$

PART 4

RESULTS AND DISCUSSION

The results of the solar organic Rankine cycle integrated with the absorption refrigeration system simulation are presented in the following chapter. Energy and exergoeconomic performance, as well as exhaustive parametric studies utilizing EES, have been conducted in this chapter. The results compare R245fa and butane as a working fluid for the ORC. In addition, the impact of operational conditions on cost and performance, which are the primary optimization objectives for this work, is examined.

4.1. MODEL VALIDATION

The validation of the ORC model involves comparing the current ORC simulation results and the model results of Delgado-Torres and García-Rodríguez [75] for R245fa, specifically for an ORC output of electricity of 100 kW and the turbine inlet temperature of 95°C. The comparison is illustrated in Table 4.1, with a consistent turbine and pump isentropic efficiency of 75%, condenser temperature of 30 °C, and regenerator efficiency of 80%. It was discovered that the current model outcomes closely resemble the findings of Delgado-Torres and García-Rodríguez [75] for the instances shown in Table 4.1. Deviation levels were relatively insignificant T_3 and η_{0RC}, but for $\dot{m}_{ORC}$, there were somewhat higher fluctuations.

Table 4.1. Verification of the ORC model by comparing the current model's findings with Ref's [75].

	Ref [75]	Present model	Deviation (%)
$T_1(°C)$	95	95	0
$\dot{m}_{ORC}$ (kg/s)	4.444	4.27	4.07
$T_3(°C)$	36.4	36.67	0.7
$\eta_{0RC}(\%)$	10.14	10.08	0.5

4.2. RESULTS OF EXERGY AND EXERGOECONOMIC AT DESIGN CONDITIONS

The current system consists of a solar Organic Rankine Cycle (ORC) with R245fa or butane integrated absorption refrigeration system using LiBr-H_2O. The exergoeconomic analysis is conducted using the input parameters provided in Table 3.1. As a result of thermodynamic and exergoeconomic analysis, the flow parameters (mass flow rate, temperature, pressure, enthalpy, exergy, and cost rate) at each state point of the present system are illustrated in Tables 4.2 and 4.3.

Table 4.2. The characteristics of the SCCHP utilizing R245fa as the working fluid for each state.

State	m (kg/s)	Fluid)	Temperature (K)	Enthalpy (kJ/kg)	Exergy (kW)	Cost ($/hr)
1	15.43	R245fa	158.5	525	1078	57.1
2	15.43	R245fa	122.1	506.9	775	41.04
3	15.43	R245fa	89.61	467.9	647	34.26
4	15.43	R245fa	89.61	323.7	249	13.19
5	15.43	R245fa	91.11	325.6	273.6	15.89
6	15.43	R245fa	115.9	364.6	399.4	23.12
7	1.821	LiBr-water	36	86.31	88.35	6.849
8	1.821	LiBr-water	36.01	86.33	88.35	6.858
9	1.821	LiBr-water	49.93	114.6	91.17	7.015
10	1.518	LiBr-water	65	203.9	196.3	10.11
11	1.518	LiBr-water	53.4	183.8	193.4	9.959
12	1.518	LiBr-water	58.34	183.8	193.3	9.962
13	0.3036	Water	65	2622	28.35	5.167
14	0.3036	Water	36.16	151.5	0.2366	0.04311
15	0.3036	Water	6.342	151.5	-1.776	0.04365
16	0.3036	Water	6.342	2513	-49.24	1.21
17	16.15	Therminol_66	70	126.1	127.6	6.235
18	16.15	Therminol_66	70.3	126.6	129	7.118
19	16.15	Therminol_66	72.3	130.1	136.8	5.746
20	16.15	Therminol_66	188.5	356.3	1091	45.84
21	16.15	Therminol_66	178.5	334.9	969.9	47.4
22	16.15	Therminol_66	101	181.6	280.3	13.7
23	53.05	Water	70	293.1	691.8	0
24	53.05	Water	80	335	1013	21.5
25	35.88	Water	30	125.7	3.112	0
26	35.88	Water	35	146.6	21.91	6148
27	34.21	Water	17	71.36	15.02	0
28	34.21	Water	12	50.41	40.81	0.787
29	42.32	Water	30	125.7	7.824	0
30	42.32	Water	35	146.6	30	4.531
31	16.15	Therminol_66	72.6	130.6	138.2	6.616

Table 4.3. The characteristics of the SCCHP utilizing butane as the working fluid for each state.

State	m (kg/s)	Fluid)	Temperature (K)	Enthalpy (kJ/kg)	Exergy (kW)	Cost ($/hr)
1	7.847	n-butane	154.6	817.4	1223	66.07
2	7.847	n-butane	120.2	782.6	926.5	50.07
3	7.847	n-butane	88.01	706.5	801.5	43.31
4	7.847	n-butane	88.01	426.5	417.2	22.54
5	7.847	n-butane	89.68	430.8	444.7	25.34
6	7.847	n-butane	114.6	506.9	567.8	32.54
7	1.894	LiBr-water	36	86.31	91.88	7.215
8	1.894	LiBr-water	36.01	86.33	91.89	7.224
9	1.894	LiBr-water	49.93	114.6	94.82	7.39
10	1.579	LiBr-water	65	203.9	204.2	10.65
11	1.579	LiBr-water	53.4	183.8	201.1	10.49
12	1.579	LiBr-water	58.34	183.8	201.1	10.49
13	0.3157	Water	65	2622	29.49	5.442
14	0.3157	Water	36.16	151.5	0.2461	0.04541
15	0.3157	Water	6.342	151.5	-1.847	0.04597
16	0.3157	Water	6.342	2513	-51.21	1.274
17	16.8	Therminol_66	70	126.2	134.5	6.667
18	16.8	Therminol_66	70.3	126.7	136	7.526
19	16.8	Therminol_66	72.3	130.2	144.1	6.123
20	16.8	Therminol_66	184.6	348.1	1087	46.19
21	16.8	Therminol_66	174.6	326.8	964.2	47.79
22	16.8	Therminol_66	101	181.7	293.4	14.54
23	52.38	Water	70	293.1	683	0
24	52.38	Water	80	335	1000	20.98
25	37.31	Water	30	125.7	3.236	0
26	37.31	Water	35	146.6	22.79	6475
27	35.58	Water	17	71.36	15.62	0
28	35.58	Water	12	50.41	42.44	0.8398
29	44.02	Water	30	125.7	8.137	0
30	44.02	Water	35	146.6	31.2	4.767
31	16.8	Therminol_66	72.6	130.7	145.6	6.968

Table 4.4 presents each system component's energy and exergy analysis for R245fa and n- butane as a working fluid for the ORC. The findings present that the ORT for the CCHP system with R245fa produces 279.7 kW, 16.77% of this power consumed by the pumps, and the work net for the system is 232.8 kW. On the other side, the CCHP system with butane produces 273 kW, 18.7% of this power consumed by the pumps, and the work net for the system is 221.83 kW. It is revealed from the table that the rate of process heat supply from the CCHP system with R245fa is 2225 kW, and it is 2197 kW for the system with butane. The rate of the heat removed from the evaporator of the CCHP system with R245fa is 716.7 kW, and it is 745.4 kW for the

system with butane. The highest rate of exegetic destruction appears by PTC solar collectors for both systems.

Table 4.4. Energy and exergy analysis for each system component for both working fluids.

Component	R245fa				n- butane			
	$\dot{E}_{D,total}$ (kW)	$\dot{E}_{D,total}$ (%)	Exergy (%)	$\dot{Q}$ or $\dot{W}$ (kW)	$\dot{E}_{D,total}$ (kW)	$\dot{E}_{D,total}$ (%)	Exergy (%)	$\dot{Q}$ or $\dot{W}$ (kW)
Absorber	33.57	0.9472	39.78	884.5	34.92	0.982	39.78	920
ARC_cond	9.32	0.263	66.86	749.4	9.7	0.2725	66.86	779.8
Boiler	10.71	0.3023	98.45	2476	16.07	0.452	97.6	2437
EV1	2.013	0.057	88.25	0	2.093	0.06	88.25	0
Evap	21.67	0.612	54.34	716.7	22.54	0.634	54.34	745.4
Generator	19.23	0.543	87.41	896.5	20.04	0.564	87.93	932.4
ORC_cond	76.75	2.166	80.71	2225	67.21	1.89	82.51	2197
ORC HE	2.305	0.0651	98.2	30.41	1.983	0.0545	98.54	597.2
ORT	23.49	0.663	92.25	279.7	23.03	0.648	92.22	273
Pump1	7.338	0.207	16.5	8.79	7.631	0.2146	16.67	9.158
Pump2	4.816	0.136	83.63	29.42	5.42	0.1524	83.57	32.98
Pump3	0.0385	0.0011	3.313	0.04	0.04	0.001	3.313	0.0414
Pump4	7.259	0.205	16.03	8.645	7.55	0.21	16.07	8.995
PRV	0.0452	0.0013	99.98	0	0.047	0.001	99.98	0
PTC	3212	90.63	22.88	4392	3223	90.63	22.6	4392
SHEX	0.1066	0.003	96.36	30.41	0.1109	0.0031	96.36	31.63
TST	113.4	3.2	88.12	3654	114.8	3.227	87.83	3661

Table 4.5 lists the results of exergoeconomic performance parameters for each component in the CCHP system for both working fluids. It is evident that the investment expenditures for the EV_1 and PRV are very insignificant when compared to other components. Consequently, their exergoeconomic factors may be considered inconsequential, resulting in a value of zero. The low exergoeconomic factor suggests that the majority of the component's overall cost is attributed to the cost of exergy destruction. To enhance the exergoeconomic efficiency of such components, it is necessary to decrease the exergy destruction cost of the component. Increasing the isentropic efficiency of power components, such as turbines, pumps, and compressors, may enhance their economic performance when the exergoeconomic variables are low. Enhancing the exergoeconomic performance of heat exchangers, including evaporators, condensers, and HXs, may be achieved by using costlier heat exchangers that provide superior heat exchange capabilities, particularly when the exergoeconomic variables are low. ORC HE in the system has the highest value of the

exergoeconomic factor because they are both fueled by superheated steam. The results indicate that the exergoeconomic factor for the system with R245fa is 72.11, while 70.86 for the system with butane. The Energy, exergy, Exergoeconomic, and environmental outcomes of the CCHP system with R245fa and butane are summarized in Table 4.6.

Table 4.5. Exergoeconomic analysis for each component of the CCHP system for both working fluids.

Component	R245fa				n- butane			
	$\dot{C}_D$ ($/h)	$\dot{Z}_K$ ($/h)	$\dot{Z}_K + \dot{C}_D$ ($/h)	f %	$\dot{C}_D$ ($/h)	$\dot{Z}_K$ ($/h)	$\dot{Z}_K + \dot{C}_D$ ($/h)	f %
Absorber	2.603	0.208	2.811	7.4	2.742	0.214	2.956	7.24
ARC_cond	1.7	0.006	1.706	0.352	1.788	0.009	1.797	0.5
Boiler	0.5236	0.2802	0.8038	34.86	0.7963	0.2837	1.08	26.27
EV1	0.367	0.0003	0.3673	0.082	0.3863	0.0006	0.3869	0.155
Evap	0.533	0.379	0.912	41.56	0.561	0.3883	0.9493	40.9
Generator	0.94	0.796	1.736	45.85	0.9933	0.8277	1.821	45.45
ORC_cond	4.065	0.426	4.491	9.486	3.632	0.217	3.849	5.64
ORC HE	0.1221	0.4444	0.5665	78.45	0.1047	0.4418	0.5465	80.84
ORT	1.244	3.866	5.11	75.66	1.244	1.686	2.93	57.54
Pump1	0.5226	0.2578	0.7804	33.03	0.4943	0.2655	0.7598	34.94
Pump2	0.25	0.6057	0.8557	70.78	0.2535	0.6592	0.9127	72.22
Pump3	0.0027	0.0056	0.00833	67.59	0.0026	0.0057	0.0083	68.67
Pump4	0.517	0.255	0.772	33.03	0.489	0.2621	0.7511	34.89
PRV	0.0023	0.0027	0.005	54	0.0024	0.0029	0.00527	54.46
PTC	0	39.22	39.22	100	0	39.22	39.22	100
SHEX	0.0055	0.0067	0.01223	55.03	0.0058	0.007	0.01275	54.67
TST	4.764	0.196	4.96	3.95	4.877	0.195	5.072	3.84
Total	18.162	46.96	65.11726	72.11	18.372	44.685	63.0576	70.86

Table 4.6. Summery of the Energy, exergy, and exergoeconomic results of the CCHP system for both organic fluids.

Working Fluid	$\dot{W}_{net}$ (kW)	$\dot{Q}_{heatin}$ (kW)	$\dot{Q}_{cooling}$ (kW)	ƞ (%)	ψ (%)	$\dot{E}_{D,total}$ kW	$\dot{C}_{total}$ $/hr	f %	CO_2 emission (kg/kWh)
R245fa	232.5	2225	716.7	86.89	16.26	3544	66.12	72.12	0.195
butane	221.8	2197	745.4	86.44	15.73	3557	63.06	70.86	0.223

4.3. PARAMETRIC STUDY

This section examines the impact of important factors, such as the superheated degree, the pressure ratio, and the solar irradiation, on the performance of the CCHP system.

4.3.1. Effect of Superheat Temperature

The net output power ($\dot{W}_{net}$) and heat rate ($\dot{Q}_{heating}$ and $\dot{Q}_{cooling}$) with the change of the superheated degree at the inlet of the ORC for the system with R245fa and butane is shown in Figure 4.1. The increase of superheated degree increases the enthalpy at the inlet of ORT which provides more $\dot{W}_{net}$ from the ORT. The heating rate ($\dot{Q}_{heating}$) also increases at the increase in the superheated degree due to the increase in the mass transfer of the working fluid through the condenser at a high superheated degree. The cooling rate ($\dot{Q}_{cooling}$) decreases at the increase in the superheated degree as a result of the reduction in the heat rate transfer to the generation at a high superheated degree.
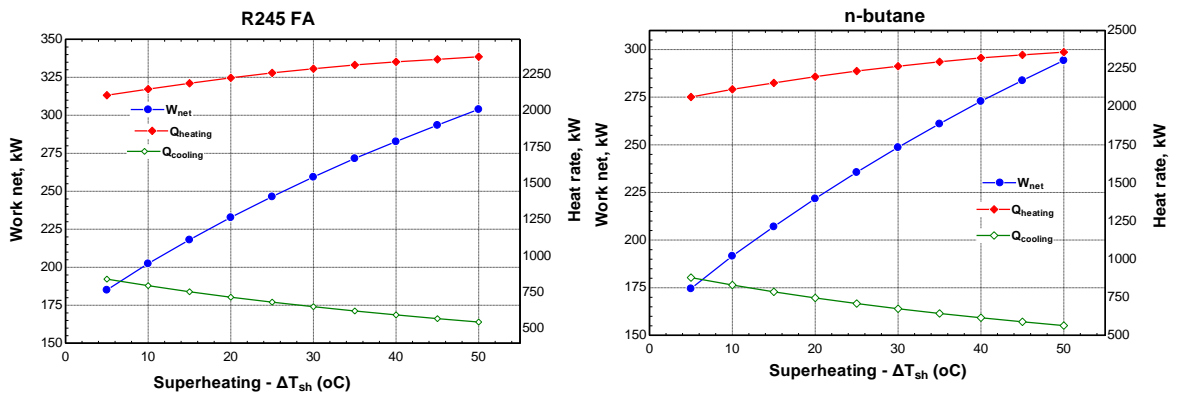

Figure 4.1. Work net, heating load, and cooling load for different superheated degree parameters.

Figure 4.2 illustrates the net output power ($\dot{W}_{net}$) and total cost rate ($\dot{C}_{Total}$) as a function of the superheated degree at the ORC intake for the system with two working fluids. The findings present that the work net increases with an increase in the superheating degree whereas the total cost decreases. The $\dot{W}_{net}$ for the CCHP system with R245fa is more significant than with butane. It is noticed from the curves when ΔT_{super} increases from 5 to 50 °C , the $\dot{W}_{net}$ increases from 174.6 to 294.3 kW for the system with butane, while it rises from 185.1 to 304 kW for the system with R245fa. Conversely, the total cost rate ($\dot{C}_{Total}$) for the CCHP system with butane is more attractive than the system with R245fa because the mass flow rate of the ORC with R245fa is higher than for the ORC with butane, and it causes an increase in the total

cost investment for the components of the ORC. The $\dot{C}_{Total}$ reduces from 66.79 to 63.69 \$/hr for the system with R245fa, while it decreases from 64.9 to 61.4 for the system with butane.
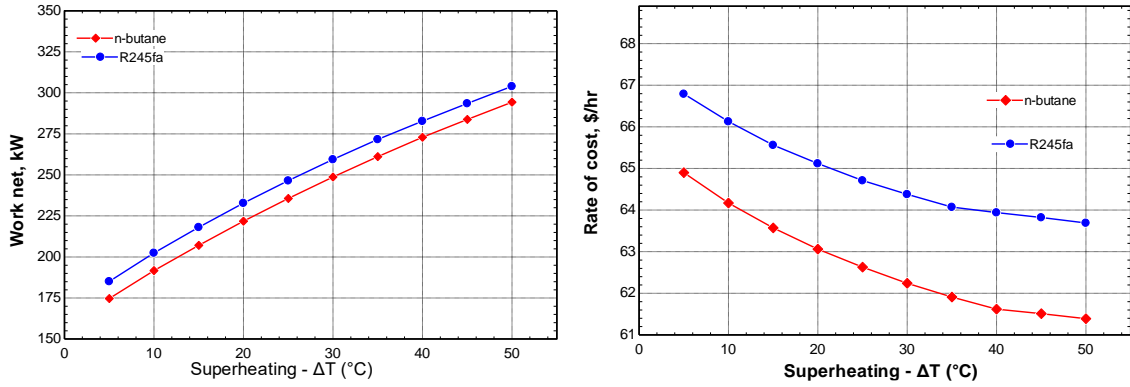

Figure 4.2. Work net and total cost rate for different superheated degree parameters.

Figure 4.3 presents the overall efficiencies of the CCHP system as a function of the superheated degree with two working fluids. It revealed from the curves both the thermal and exergy efficiency of the system increased with an increase in the ΔT_{super} due to the enhancement of the system output ($\dot{W}_{net}$ and $\dot{Q}_{heating}$) at high ΔT_{super}. In comparison to the butane -based system, the CCHP system that uses R245fa achieves higher overall efficiency. The $\eta_{thermal}$ enhances from 85.13 to 89.5 % and the η_{exergy} increases from 14.8 to 18.32 % for the system with R245fa when ΔT_{super} increases from 5 to 50 °C. Also, the $\eta_{thermal}$ enhances from 84.59 to 89.21 % and the η_{exergy} increases from 14.25 to 17.85 % for the system with butane.
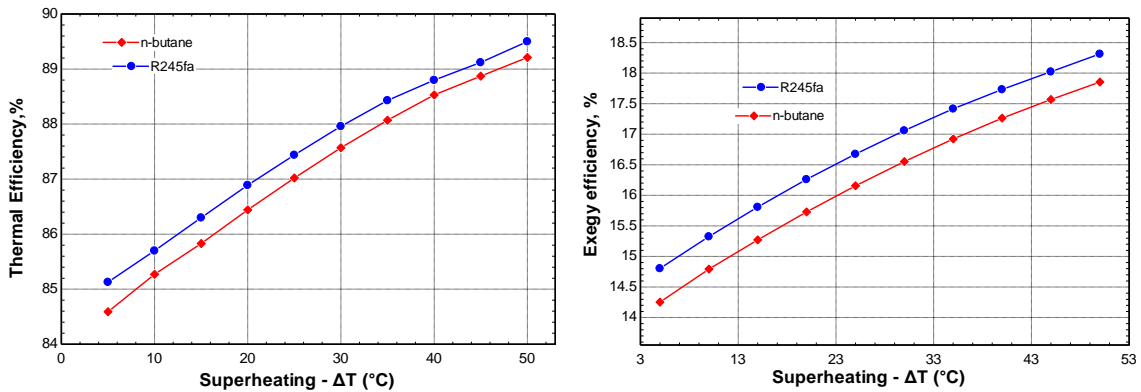

Figure 4.3. Overall efficiencies of the CCHP system for different superheated degree parameters.

Figure 4.4 shows the effect of an increase in the superheated degree from 5°C to 50°C on the exergy destruction of the CCHP system with two working fluids. Higher ΔT_{super} results in increased exergy destruction within the ORC components, but the exergy destruction in the PTC, TST, and ARC components reduces and course to a reduction in the exergy destruction for the CCHP system in general as seen in figure 4.4. The $\dot{E}_{D,total}$ reduces from 3610 kW to 3478 kW for the system with butane when ΔT_{super} increases from 5 to 50 °C. Also, the $\dot{E}_{D,total}$ diminishes 3597 kW to 3468 kW with R245fa. The reduction in the $\dot{E}_{D,total}$ enhances the exergy efficiency of the system as shown in figure 4.3. In addition, the exergy efficiency of the R245fa system is higher than that of the butane system since its $\dot{E}_{D,total}$ is lower.
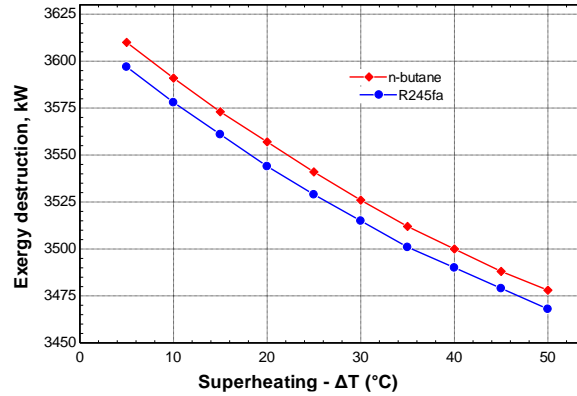

Figure 4.4. Total exergy destruction of the CCHP system for different superheated degree parameters.

4.3.2. Effect of Pressure Ratio Parameters

The pressure ratio (α) represents the relationship between the turbine intake pressure (P_1) and the critical pressure ($P_{critical}$) of the working fluid. For R245fa, the critical pressure is 3651 kPa, whereas for butane, it is 3797 kPa.

Fig. 4.5 illustrates the effect of the change of pressure ratio on the net output power ($\dot{W}_{net}$) and heat rate ($\dot{Q}_{heating}$ and $\dot{Q}_{cooling}$) for the CCHP system with R245fa and butane. The curves presents that the effect of the pressure ratio on the $\dot{W}_{net}$, $\dot{Q}_{heating}$ and $\dot{Q}_{cooling}$ is like the effect of the superheat degree. $\dot{W}_{net}$ and $\dot{Q}_{heating}$ increase with an increase in the pressure ratio whereas the $\dot{Q}_{cooling}$ reduces.
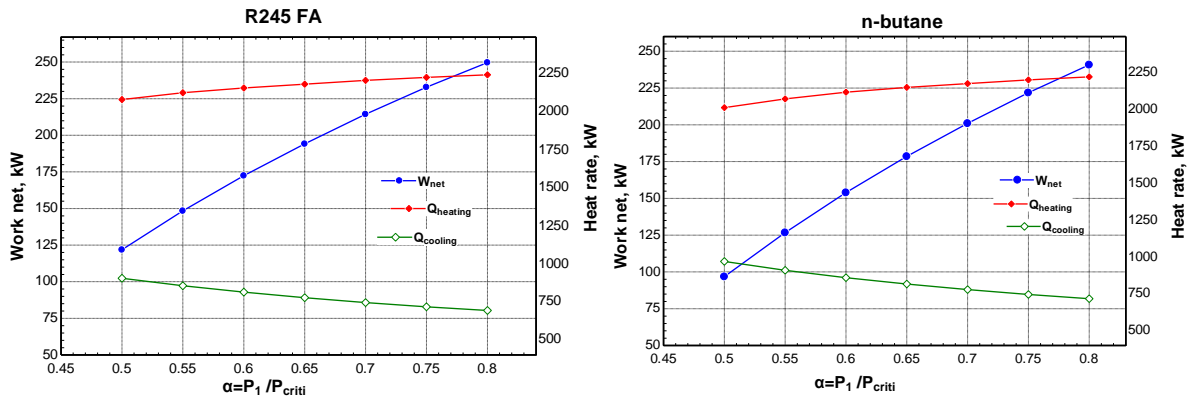
Figure 4.5. Work net, heating load, and cooling load for different pressure ratio parameters.

The effect of the pressure ratio parameter on the $\dot{W}_{net}$ and $\dot{C}_{Total}$ of the CCHP system are shown in Figure 4.6. The results indicate that the $\dot{W}_{net}$ rises as the pressure ratio increases, but the overall cost $\dot{C}_{Total}$ reduces. The $\dot{W}_{net}$ production of the CCHP system using R245fa is higher, while the overall cost $\dot{C}_{Total}$ is more expensive than using butane. It can be seen from the graphs that when the $\propto$ value goes from 0.5 to 0.8, the $\dot{W}_{net}$ increases from 96.83 kW to 240.8 kW for the system using butane, and from 121.8 kW to 249.6 kW for the system using R245fa. The $\dot{C}_{Total}$ reduces from 68.67 \$/hr to 64.74 \$/hr for the system with R245fa, while it decreases from 68.61\$/hr to 62.46 \$/hr for the system with butane.
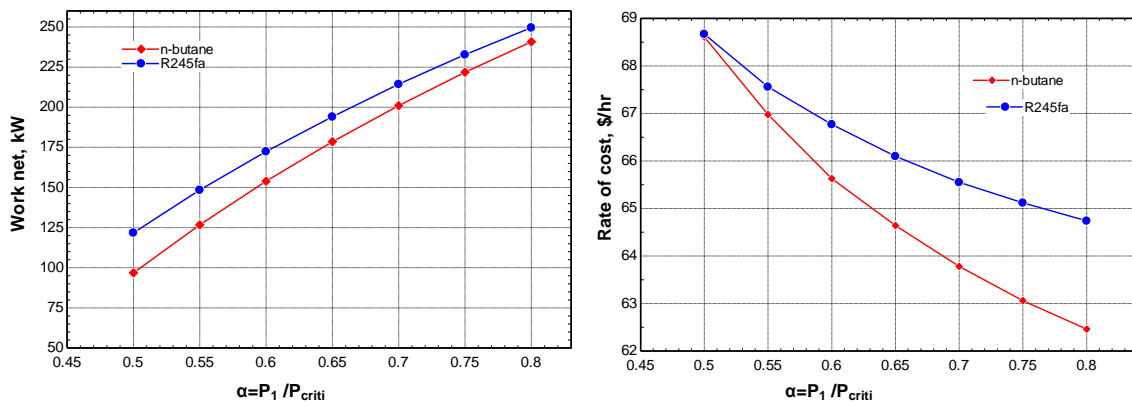

Figure 4.6. Work net and total cost rate for different pressure ratio parameters.

The overall efficiencies of the system as a function of the pressure ratio with two working fluids are presented in Figure 4.7. At a high-pressure ratio ($\propto$), the $\dot{W}_{net}$ and

$\dot{Q}_{heating}$ increase and cause an enhancement in the overall efficiencies of the system for both fluids. The CCHP system with R245fa demonstrates superior overall efficiency as compared to the butane -based system. When the pressure ratio ($\propto$) increases from 0.5 to 0.8, the $\eta_{thermal}$ improves from 84.19 to 87.28% and the η_{exergy} increases from 13.28 to 16.7% for the system using R245fa. Similarly, for the system using butane, the $\eta_{thermal}$ increases from 83.13 to 86.89% % and the η_{exergy} increases from 12.3 to 16.23%.
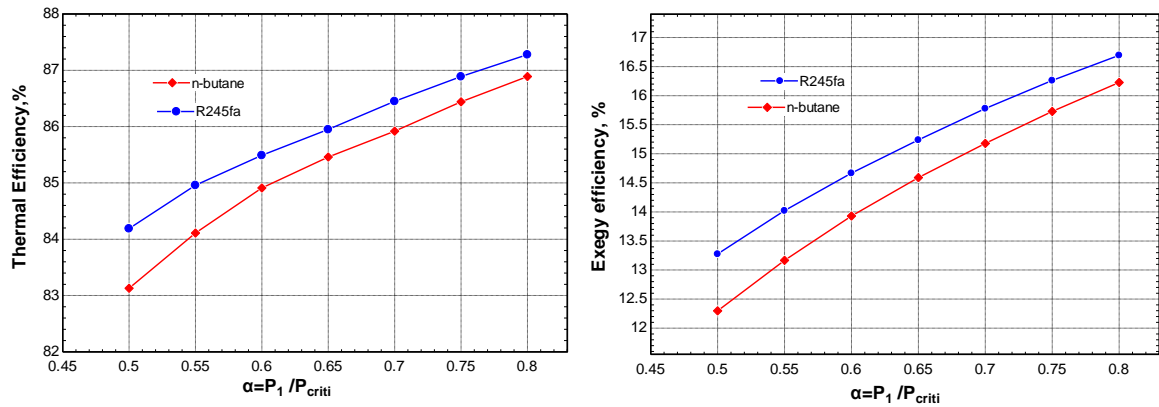
Figure 4.7. Overall efficiencies of the system for different pressure ratio parameters.

The impact of an increase in the pressure ratio from 0.5 to 0.8 on the total exergy destruction of the system with two working fluids is illustrated in Figure 4.8. Greater pressure (Pr) increases exergy destruction in the ORT and ORC condenser. However, the exergy destruction in the PTC, TST, boiler, and ARC components decreases, resulting in an overall reduction in exergy destruction for the CCHP system, as displayed in Figure 4.8. The $\dot{E}_{D,total}$ decreases from 3688 kW to 3537 kW as the Pr rises from 0.5 to 0.8 in the system using butane. Furthermore, the overall rate of energy destruction decreases from 3659 kW to 3527 kW while using R245fa as a working fluid.
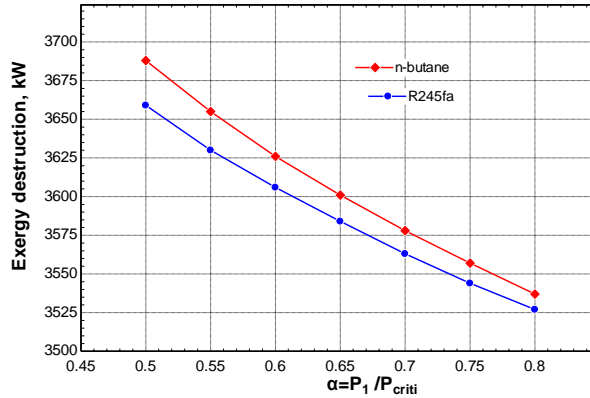
Figure 4.8. Exergy destruction of the system for various pressure ratio factors.

4.3.3. Effect of Sollar Irradiation

The effect of solar irradiation (G_B) on the performance of the CCHP system such as $\dot{W}_{net}$, $\dot{Q}_{heating}$, $\dot{Q}_{cooling}$, $\eta_{thermal}$, η_{exergy}, and $\dot{E}_{D,total}$ are represented in the Figures 4.9- 4.12. Figure 4.8 demonstrates how the change in solar irradiation impacts the $\dot{W}_{net}$, $\dot{Q}_{heating}$, and $\dot{Q}_{cooling}$ of the CCHP system using R245fa and butane. The charts demonstrate that the increase in the solar irradiation enhances the $\dot{W}_{net}$, $\dot{Q}_{heating}$ and $\dot{Q}_{cooling}$ of the system. At high solar irradiation, the mass flow rate of the fluid through the ORC increases and boosts the $\dot{W}_{net}$ and $\dot{Q}_{heating}$ of the system. Also, the heat transfer to the generation increases and improves the performance of the ARC and the $\dot{Q}_{cooling}$ of the system.

Figure 4.9. Work net, heating load, and cooling load for different solar irradiation.

43

Figure 4.10 reveals the $\dot{W}_{net}$ and total cost rate $\dot{C}_{Total}$ as a function of the intensive solar irradiation for the system with two working fluids. The findings present that the work net increases with an increase in solar irradiation and that the overall cost rate increases, too. At high solar irradiation, the amount of thermal energy transferred to the system rises, and the mass flow rate of the working flui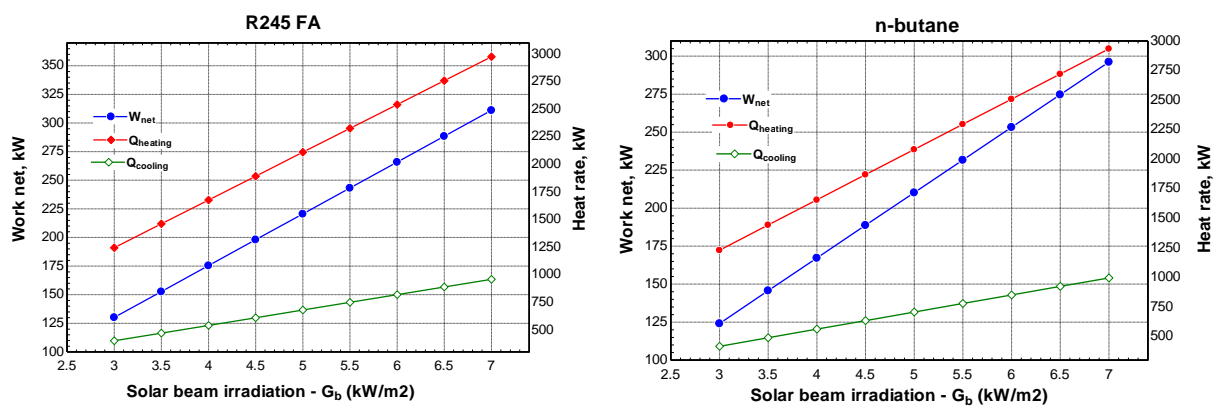ds increases which causes an increase in the outputs from the system. The overall cost of the system increases due to the increase in the capacity for each system's component at a high mass flow rate. It is observed from the curves when G_B increases from 3 to 7 kW/m^2, the $\dot{W}_{net}$ increases from 124.1 to 296.2 kW for the system with butane, while it rises from 130.1 to 311.1kW for the system with R245fa. The $\dot{C}_{Total}$ also increases from 61.51 to 66.78 \$/hr for the system with R245fa, while it rises from 60.55 to 64.88 for the system with butane.
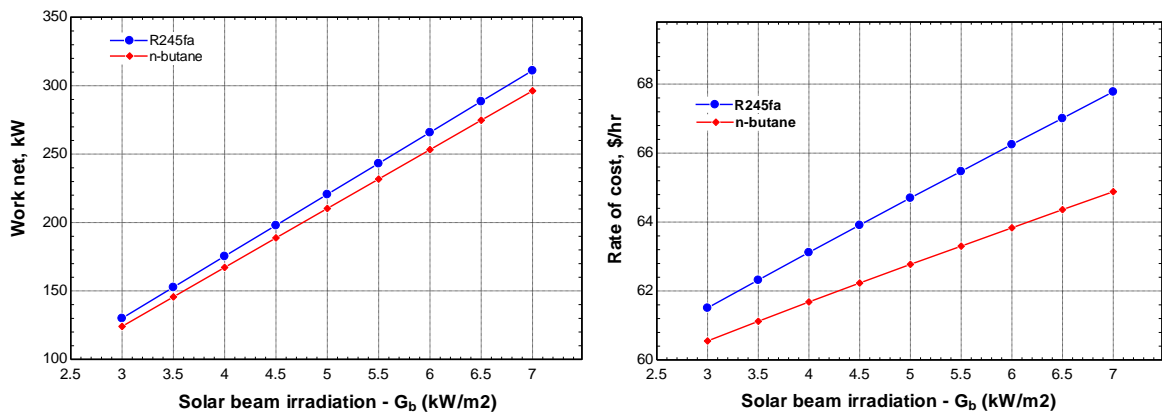
Figure 4.10. Work net and total cost rate for different solar irradiation.

The change in the overall efficiencies of the system for different solar irradiation with two working fluids are showed in Figure 4.11. The $\eta_{thermal}$ remains constant for different solar irradiation for the system with various working fluids because the energy input and output from the system grow proportionally as the solar irradiation increases. The $\eta_{thermal}$ for the system with R245fa remains at 86.89%, while it's 86.44% for the system with butane. As the solar irradiation increases, the exergy input to the system rises, leading to a modest improvement in the system's η_{exergy}. When G_B increases from 3 to 7 kW/m^2, the η_{exergy} improves from 15.97 to 16.36% for the system using R245fa and it improves from 15.46 to 15.82% for the system using octane.
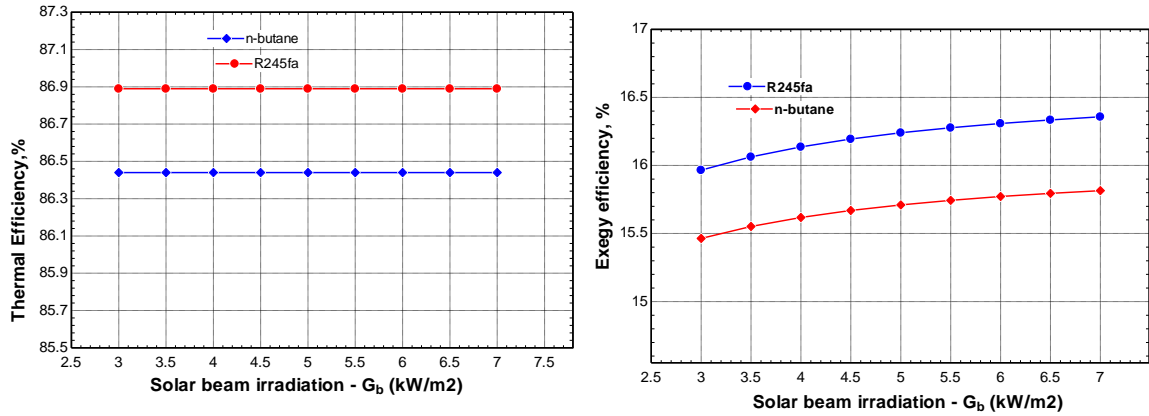
Figure 4.11. Overall efficiencies of the system for different solar irradiation.

The influence of an increase in the solar irradiation from 3 to 7 kW/m^2 on the total exergy destruction of the system with two working fluids is presented in Figure 4.12. The total exergy destruction for the CCHP system rises with high solar irradiation, as shown in Figure 4.11 since the exergy destruction for all components in the system increases. The exergy destruction for the system with both fluids is very close. In the butane system, the $\dot{E}_{D,total}$ grows from 2030 to 4720 kW when the G_b increases from 3 to 7 kW/m^2. In addition, when R245fa is used as a working fluid, the total rate of energy destruction increases from 2024 kW to 47033 kW.
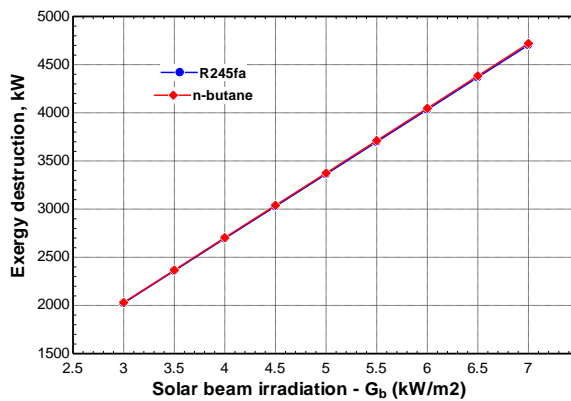
Figure 4.11. The total exergy destruction of the system for different solar irradiation.

PART 5

CONCLUSION

The objective of this study is to examine a solar-powered trigeneration system capable of producing electricity, heating, and cooling. The system is specifically designed to be compatible with the conditions and requirements of operating in the geographical location of Antalya, Turkey. The proposed system utilizes PTC collectors with Therminol 66 and incorporates an organic Rankine cycle, an absorption refrigeration system, and a thermal storage tank. The findings achieved a comparison between the system's operation utilizing two different working fluids for ORC. These working fluids are R245fa and butane. The system undergoes energy, exergy, and exergoeconomic analysis to determine the most efficient performance and cost. The study is conducted using a model created using Engineering Equation Solver (EES). Outlined below are the main findings of this study:

- Under optimal design parameters, the CCHP system with R245fa has an electricity output of 232.5 kW, cooling production of 716.7 kW, heating production of 2225 Kw, thermal efficiency of 86.89%, exergy efficiency of 16.26%, and an overall cost rate of 66.12 $/h, and the exergoeconomic factor is 72.12%. The CCHP system with octane has an electrical output of 221.8 kW, cooling production of 745.4 kW, heating production of 2197 kW, thermal efficiency of 86.44%, exergy efficiency of 15.73%, an overall cost rate of 63.06 $/h, and the exergoeconomic factor is 70.86%.
- The increase in the superheated degree increases the electricity output and heating production while decreasing the cooling production and total cost rate. Also, thermal and exergy efficiencies increase at a high superheated degree.
- Higher pressure ratios result in increased power output and heating production, but decreased cooling production and overall cost rate. Furthermore, elevated pressure ratios lead to a rise in both thermal and exergy efficiency.

- Increasing solar irradiation increases electricity production, cooling, and heating production. However, it also results in a rise in the overall cost rate. Furthermore, exergy efficiencies exhibit an upward trend in response to increased solar irradiation, while the thermal efficiency stays consistent.

- The CCHP system using R245fa demonstrates greater performance in comparison to the system using octane.

- The highest rate of exegetic destruction appears by PTC solar collectors for both systems.

- The carbon footprint of the CCHP system using R245fa is more favorable than the system that utilizes octane.

REFERENCES

1. Shaaban, M. and Petinrin, J. O., "Renewable energy potentials in Nigeria: Meeting rural energy needs", *Renewable And Sustainable Energy Reviews*, 29: 72–84 (2014).

2. Liu, M., Shi, Y., and Fang, F., "Combined cooling, heating and power systems: A survey", *Renewable And Sustainable Energy Reviews*, 35: 1–22 (2014).

3. Karduri, R., Karduri, R. K. R., and Advisor, A., "Integrating Renewable Energy into Existing Power Systems: Challenges and Opportunities", *International Journal Of Advanced Research In Management*, IV (March 2018): (2018).

4. Rashid, F. L., Eleiwi, M. A., Mohammed, H. I., Ameen, A., and Ahmad, S., "A Review of Using Solar Energy for Cooling Systems: Applications, Challenges, and Effects", *Energies*, 16 (24): (2023).

5. Talal, W. and Akroot, A., "Exergoeconomic Analysis of an Integrated Solar Combined Cycle in the Al-Qayara Power Plant in Iraq", *Processes*, 11 (3): (2023).

6. Kazem, H. A. and Chaichan, M. T., "Status and future prospects of renewable energy in Iraq", *Renewable And Sustainable Energy Reviews*, 16 (8): 6007–6012 (2012).

7. Dawood, T. A., Raphael, R., Barwari, I., and Akroot, A., "Solar Energy and Factors Affecting the Efficiency and Performance of Panels in Erbil / Kurdistan", *International Journal Of Heat And Technology*, 41 (2): 304–312 (2023).

8. Kannan, N. and Vakeesan, D., "Solar energy for future world: - A review", *Renewable And Sustainable Energy Reviews*, 62: 1092–1105 (2016).

9. Xie, W. T., Dai, Y. J., Wang, R. Z., and Sumathy, K., "Concentrated solar energy applications using Fresnel lenses: A review", *Renewable And Sustainable Energy Reviews*, 15 (6): 2588–2606 (2011).

10. Hassanien, R. H. E., Li, M., and Dong Lin, W., "Advanced applications of solar energy in agricultural greenhouses", *Renewable And Sustainable Energy Reviews*, 54: 989–1001 (2016).

11. Green, M. A., Ho-Baillie, A., and Snaith, H. J., "The emergence of perovskite solar cells", *Nature Photonics*, 8 (7): 506–514 (2014).

12. Kabir, E., Kumar, P., Kumar, S., Adelodun, A. A., and Kim, K. H., "Solar energy: Potential and future prospects", *Renewable And Sustainable Energy Reviews*, 82 (August 2017): 894–900 (2018).

13. Jebasingh, V. K. and Herbert, G. M. J., "A review of solar parabolic trough collector", *Renewable And Sustainable Energy Reviews*, 54: 1085–1091 (2016).

14. Ahmad, A., Prakash, O., Kausher, R., Kumar, G., Pandey, S., and Hasnain, S. M. M., "Parabolic trough solar collectors: A sustainable and efficient energy source", *Materials Science For Energy Technologies*, 7 (August 2023): 99–106 (2024).

15. Manikandan, G. K., Iniyan, S., and Goic, R., "Enhancing the optical and thermal efficiency of a parabolic trough collector – A review", *Applied Energy*, 235 (November 2018): 1524–1540 (2019).

16. González-Roubaud, E., Pérez-Osorio, D., and Prieto, C., "Review of commercial thermal energy storage in concentrated solar power plants: Steam vs. molten salts", *Renewable And Sustainable Energy Reviews*, 80 (February): 133–148 (2017).

17. Bellos, E., Tzivanidis, C., and Antonopoulos, K. A., "A detailed working fluid investigation for solar parabolic trough collectors", *Applied Thermal Engineering*, 114: 374–386 (2017).

18. Nawaf, M. Y., Akroot, A., and Wahhab, H. A. A., "Numerical simulation of a porous media solar collector integrated with thermal energy storage system", (2023).

19. Cabrera, F. J., Fernández-García, A., Silva, R. M. P., and Pérez-García, M., "Use of parabolic trough solar collectors for solar refrigeration and air-conditioning applications", *Renewable And Sustainable Energy Reviews*, 20: 103–118 (2013).

20. Colonna, P., Casati, E., Trapp, C., Mathijssen, T., Larjola, J., Turunen-Saaresti, T., and Uusitalo, A., "Organic Rankine Cycle Power Systems: From the Concept to Current Technology, Applications, and an Outlook to the Future", *Journal Of Engineering For Gas Turbines And Power*, 137 (10): (2015).

21. Bdaiwi, M., Akroot, A., Wahhab, H. A. A., and Mahariq, I., "Numerical analysis of the steam turbine performance in power station with a low power cycle", (2023).

22. Rettig, A., Lagler, M., Lamare, T., Li, S., Mahadea, V., Mccallion, S., and Chernushevich, J., "Application of Organic Rankine Cycles (ORC)", *World Engineers' Convention*, 1–10 (2011).

23. Rahbar, K., Mahmoud, S., Al-Dadah, R. K., Moazami, N., and Mirhadizadeh, S. A., "Review of organic Rankine cycle for small-scale applications", *Energy Conversion And Management*, 134: 135–155 (2017).

24. Xu, Z. Y. and Wang, R. Z., "Absorption refrigeration cycles: Categorized based on the cycle construction", *International Journal Of Refrigeration*, 62: 114–136 (2016).

25. Khudhur, J., Akroot, A., and Al-samari, A., "Experimental Investigation of Direct Solar Photovoltaics that Drives Absorption Refrigeration System", *Journal Of*

Advanced Research In Fluid Mechanics And Thermal Sciences, 1 (1): 116–135 (2023).

26. Talal, W. and Akroot, A., "An Exergoeconomic Evaluation of an Innovative Polygeneration System Using a Solar-Driven Rankine Cycle Integrated with the Al-Qayyara Gas Turbine Power Plant and the Absorption Refrigeration Cycle", *Machines*, 12 (2): 133 (2024).

27. Chen, Y., Han, W., and Jin, H., "Thermodynamic performance optimization of the absorption-generation process in an absorption refrigeration cycle", *Energy Conversion And Management*, 126: 290–301 (2016).

28. Lima, A. A. S., Leite, G. de N. P., Ochoa, A. A. V., Dos Santos, C. A. C., da Costa, J. A. P., Michima, P. S. A., and Caldas, A. M. A., "Absorption refrigeration systems based on ammonia as refrigerant using different absorbents: Review and applications", *Energies*, 14 (1): (2021).

29. Koehler, J., Tegethoff, W. J., Westphalen, D., and Sonnekalb, M., "Absorption refrigeration system for mobile applications utilizing exhaust gases", *International Communications In Heat And Mass Transfer*, 32 (5): 333–340 (1997).

30. Wang, J., Li, S., Zhang, G., and Yang, Y., "Performance investigation of a solar-assisted hybrid combined cooling, heating and power system based on energy, exergy, exergo-economic and exergo-environmental analyses", *Energy Conversion And Management*, 196 (June): 227–241 (2019).

31. Wang, J., Chen, Y., and Lior, N., "Exergo-economic analysis method and optimization of a novel photovoltaic/thermal solar-assisted hybrid combined cooling, heating and power system", *Energy Conversion And Management*, 199 (June): 111945 (2019).

32. Wang, J., Han, Z., and Guan, Z., "Hybrid solar-assisted combined cooling, heating, and power systems: A review", *Renewable And Sustainable Energy Reviews*, 133 (August): 110256 (2020).

33. Fani, M. and Sadreddin, A., "Solar assisted CCHP system, energetic, economic and environmental analysis, case study: Educational office buildings", *Energy And Buildings*, 136: 100–109 (2017).

34. Ukaegbu, U., Tartibu, L., and Lim, C. W., "Multi-Objective Optimization of a Solar-Assisted Combined Cooling, Heating and Power Generation System Using the Greywolf Optimizer", *Algorithms*, 16 (10): (2023).

35. Liu, J., Ren, J., Zhang, Y., Huang, W., Xu, C., and Liu, L., "Exergoeconomic Evaluation of a Cogeneration System Driven by a Natural Gas and Biomass Co-Firing Gas Turbine Combined with a Steam Rankine Cycle, Organic Rankine Cycle, and Absorption Chiller", *Processes*, 12 (1): 82 (2023).

36. Gao, Q., Zhao, S., Zhang, Z., Zhang, J., Zhao, Y., Sun, Y., Li, D., and Yuan, H., "Performance Analysis and Multi-Objective Optimization of a Cooling-Power-

Desalination Combined Cycle for Shipboard Diesel Exhaust Heat Recovery", *Sustainability*, 15 (24): 16942 (2023).

37. Wang, H., Wang, J., Liu, Z., Chen, H., and Liu, X., "Thermodynamic Analysis of a New Combined Cooling and Power System Coupled by the Kalina Cycle and Ammonia–Water Absorption Refrigeration Cycle", *Sustainability (Switzerland)*, 14 (20): (2022).

38. Zeng, J., Li, Z., and Peng, Z., "Exergoeconomic analysis and optimization of solar assisted hybrid cooling systems in full working conditions", *Applied Thermal Engineering*, 206 (July 2021): 118082 (2022).

39. Divan, A., Zahedi, A., and Mousavi, S. S., "Conceptual design and technical analysis of a hybrid natural gas/molten carbonate fuel cell system for combined cooling, heating, and power applications", *Energy And Buildings*, 273: 112402 (2022).

40. Rostamnejad Takleh, H., Zare, V., Mohammadkhani, F., and Sadeghiazad, M. M., "Proposal and thermoeconomic assessment of an efficient booster-assisted CCHP system based on solar-geothermal energy", *Energy*, 246: 123360 (2022).

41. Wang, J., Wang, J., Yang, X., Xie, K., and Wang, D., "A novel emergy-based optimization model of a building cooling, heating and power system", *Energy Conversion And Management*, 268 (March): 115987 (2022).

42. Pokson, C. and Chaiyat, N., "Thermal performance of a combined cooling, heating, and power (CCHP) generation system from infectious medical waste", *Case Studies In Chemical And Environmental Engineering*, 6 (June): (2022).

43. Pilou, M., Kosmadakis, G., Meramveliotakis, G., and Krikas, A., "Towards a 100% renewable energy share for heating and cooling in office buildings with solar and geothermal energy", *Solar Energy Advances*, 2 (May): 100020 (2022).

44. Zisopoulos, G., Nesiadis, A., Atsonios, K., Nikolopoulos, N., Stitou, D., and Coca-Ortegón, A., "Conceptual design and dynamic simulation of an integrated solar driven thermal system with thermochemical energy storage for heating and cooling", *Journal Of Energy Storage*, 41 (July): (2021).

45. Khalid Shaker Al-Sayyab, A., Mota-Babiloni, A., and Navarro-Esbrí, J., "Novel compound waste heat-solar driven ejector-compression heat pump for simultaneous cooling and heating using environmentally friendly refrigerants", *Energy Conversion And Management*, 228 (December 2020): (2021).

46. Yan, R., Lu, Z., Wang, J., Chen, H., Wang, J., Yang, Y., and Huang, D., "Stochastic multi-scenario optimization for a hybrid combined cooling, heating and power system considering multi-criteria", *Energy Conversion And Management*, 233 (November 2020): 113911 (2021).

47. Ao, X., Liu, J., Hu, M., Zhao, B., and Pei, G., "A rigid spectral selective cover for integrated solar heating and radiative sky cooling system", *Solar Energy Materials And Solar Cells*, 230 (July): 111270 (2021).

48. Wang, J., Han, Z., Liu, Y., Zhang, X., and Cui, Z., "Thermodynamic analysis of a combined cooling, heating, and power system integrated with full-spectrum hybrid solar energy device", *Energy Conversion And Management*, 228 (October 2020): 113596 (2021).

49. Nami, H., Anvari-Moghaddam, A., and Nemati, A., "Modeling and analysis of a solar boosted biomass-driven combined cooling, heating and power plant for domestic applications", *Sustainable Energy Technologies And Assessments*, 47 (June): 101326 (2021).

50. Cavalcanti, E. J. C., Ferreira, J. V. M., and Carvalho, M., "Exergy assessment of a solar-assisted combined cooling, heat and power system", *Sustainable Energy Technologies And Assessments*, 47 (June): (2021).

51. Wang, J., Qi, X., Ren, F., Zhang, G., and Wang, J., "Optimal design of hybrid combined cooling, heating and power systems considering the uncertainties of load demands and renewable energy sources", *Journal Of Cleaner Production*, 281: 125357 (2021).

52. Wang, J., Ma, C., and Wu, J., "Thermodynamic analysis of a combined cooling, heating and power system based on solar thermal biomass gasification☆", *Applied Energy*, 247 (April): 102–115 (2019).

53. Saini, P., Singh, J., and Sarkar, J., "Thermodynamic, economic and environmental analyses of a novel solar energy driven small-scale combined cooling, heating and power system", *Energy Conversion And Management*, 226 (October): 113542 (2020).

54. Ramos, A., Chatzopoulou, M. A., Guarracino, I., Freeman, J., and Markides, C. N., "Hybrid photovoltaic-thermal solar systems for combined heating, cooling and power provision in the urban environment", *Energy Conversion And Management*, 150: 838–850 (2017).

55. Akroot, A. and Nadeesh, A., "Performance Analysis of Hybrid Solid Oxide Fuel Cell-Gas Turbine Power System", (2021).

56. Akroot, A., "Effect of Operating Temperatures on the Performance of a SOFCGT Hybrid System", *International Journal Of Trend In Scientific Research And Development*, Volume-3 (Issue-3): 1512–1515 (2019).

57. Akroot, A. and Namli, L., "Performance assessment of an electrolyte-supported and anode-supported planar solid oxide fuel cells hybrid system", *J Ther Eng*, 7 (7): 1921–1935 (2021).

58. Kareem, A. F., Akroot, A., Abdul Wahhab, H. A., Talal, W., Ghazal, R. M., and Alfaris, A., "Exergo–Economic and Parametric Analysis of Waste Heat Recovery from Taji Gas Turbines Power Plant Using Rankine Cycle and Organic Rankine Cycle", *Sustainability (Switzerland)*, 15 (12): (2023).

59. Besevli, B., Kayabasi, E., Akroot, A., Talal, W., Alfaris, A., Assaf, Y. H., Nawaf, M. Y., Bdaiwi, M., and Khudhur, J., "Technoeconomic Analysis of Oxygen-Supported Combined Systems for Recovering Waste Heat in an Iron-Steel Facility", *Applied Sciences*, 14 (6): 2563 (2024).

60. Akroot, A. and Al Shammre, A. S., "Techno-Economic and Environmental Impact Analysis of a 50 MW Solar-Powered Rankine Cycle System", *Processes*, 12 (6): 1059 (2024).

61. Khoshgoftar Manesh, M. H., Mousavi Rabeti, S. A., Nourpour, M., and Said, Z., "Energy, exergy, exergoeconomic, and exergoenvironmental analysis of an innovative solar-geothermal-gas driven polygeneration system for combined power, hydrogen, hot water, and freshwater production", *Sustainable Energy Technologies And Assessments*, 51 (April 2021): (2022).

62. Elmorsy, L., Morosuk, T., and Tsatsaronis, G., "Comparative exergoeconomic evaluation of integrated solar combined-cycle (ISCC) configurations", *Renewable Energy*, 185: 680–691 (2022).

63. Bakhshmand, S. K., Saray, R. K., Bahlouli, K., Eftekhari, H., and Ebrahimi, A., "Exergoeconomic analysis and optimization of a triple-pressure combined cycle plant using evolutionary algorithm", *Energy*, 93: 555–567 (2015).

64. Wu, C., Wang, S. sen, Feng, X. jia, and Li, J., "Energy, exergy and exergoeconomic analyses of a combined supercritical CO2 recompression Brayton/absorption refrigeration cycle", *Energy Conversion And Management*, 148: 360–377 (2017).

65. Sun, L., Wang, D., and Xie, Y., "Energy, exergy and exergoeconomic analysis of two supercritical CO2 cycles for waste heat recovery of gas turbine", *Applied Thermal Engineering*, 196 (July): 117337 (2021).

66. Shokati, N., Mohammadkhani, F., Yari, M., Mahmoudi, S. M. S., and Rosen, M. A., "A comparative exergoeconomic analysis of waste heat recovery from a gas turbine-modular helium reactor via organic rankine cycles", *Sustainability (Switzerland)*, 6 (5): 2474–2489 (2014).

67. Han, Z., Wang, J., Cui, Z., Lu, C., and Qi, X., "Multi-objective optimization and exergoeconomic analysis for a novel full-spectrum solar-assisted methanol combined cooling, heating, and power system", *Energy*, 237: 121537 (2021).

68. Dhahad, H. A., Ahmadi, S., Dahari, M., Ghaebi, H., and Parikhani, T., "Energy, exergy, and exergoeconomic evaluation of a novel CCP system based on a solid oxide fuel cell integrated with absorption and ejector refrigeration cycles", *Thermal Science And Engineering Progress*, 21 (May 2020): 100755 (2021).

69. Xie, N., Xiao, Z., Du, W., Deng, C., Liu, Z., and Yang, S., "Thermodynamic and exergoeconomic analysis of a proton exchange membrane fuel cell/absorption chiller CCHP system based on biomass gasification", *Energy*, 262 (PB): 125595 (2023).

70. Akrami, E., Nemati, A., Nami, H., and Ranjbar, F., "Exergy and exergoeconomic assessment of hydrogen and cooling production from concentrated PVT equipped with PEM electrolyzer and LiBr-H2O absorption chiller", *International Journal Of Hydrogen Energy*, 43 (2): 622–633 (2018).

71. Nourpour, M. and Khoshgoftar Manesh, M. H., "Evaluation of novel integrated combined cycle based on gas turbine-SOFC-geothermal-steam and organic Rankine cycles for gas turbo compressor station", *Energy Conversion And Management*, 252: (2022).

72. Cavalcanti, E. J. C., .

73. Pierobon, L., Nguyen, T. Van, Larsen, U., Haglind, F., and Elmegaard, B., "Multi-objective optimization of organic Rankine cycles for waste heat recovery: Application in an offshore platform", *Energy*, 58: 538–549 (2013).

74. Khaljani, M., Khoshbakhti Saray, R., and Bahlouli, K., "Comprehensive analysis of energy, exergy and exergo-economic of cogeneration of heat and power in a combined gas turbine and organic Rankine cycle", *Energy Conversion And Management*, 97: 154–165 (2015).

75. Delgado-Torres, A. M. and García-Rodríguez, L., "Analysis and optimization of the low-temperature solar organic Rankine cycle (ORC)", *Energy Conversion And Management*, 51 (12): 2846–2856 (2010).

RESUME

Muhamad REFAAI is a mechanical engineer who graduated from the faculty of Engineering, University of Karabük – TURKEY, and obtained his bachelor's degree in 2020. He is currently studying for his master's degree at Karabük University, Department of Mechanical Engineering.